Ocean Sci. J. (2013) 48(1):69-97
http://dx.doi.org/10.1007/s12601-013-0007-0
Available online at http://link.springer.com
SpringerLink
Ocean Science Journal

Review

An Overview of Developments and Applications of Oceanographic Radar Networks in Asia and Oceania Countries

Satoshi Fujii[1], Malcolm L. Heron[2], Kuh Kim[3]*, Jian-Wu Lai[4], Sang-Ho Lee[5], Xiangbai Wu[6], Xiongbin Wu[7], Lucy R. Wyatt[2], and Wen-Chang Yang[4]

[1]*Department of Electrical and Electronics Engineering, University of the Ryukyus, Okinawa 903-0213, Japan*
[2]*ACORN, TropWATER and AIMS@JCU, James Cook University, Townsville, Queensland 4811, Australia*
[3]*Research Institute of Oceanography, Seoul National University, Seoul 151-742, Korea*
[4]*Taiwan Ocean Research Institute, National Applied Research Laboratories, Kaohsiung 852, Taiwan*
[5]*Department of Oceanography, Kunsan National University, Gunsan 573-701, Korea*
[6]*State Key Laboratory of Marine Environmental Science, College of Ocean and Earth Sciences, Xiamen University, Xiamen 361102, China*
[7]*School of Electronic Information, Wuhan University, Wuhan 430072, China*

Received 25 January 2013; Revised 28 February 2013; Accepted 11 March 2013

Abstract – More than 110 radar stations are in operation at the present time in Asia and Oceania countries, which is nearly half of all the existing radar stations in the world, for purposes related to marine safety, oil spill response, tsunami warning, coastal zone management and understanding of ocean current dynamics, depending mainly on each country's coastal sea characteristics. This paper introduces the oceanographic radar networks of Australia, China, Japan, Korea and Taiwan, presented at the 1st Ocean Radar Conference for Asia (ORCA) held in May 2012, Seoul, Korea, to share information about the radar network developments and operations, knowledge and experiences of data management, and research activity and application of the radar-derived data of neighbouring countries. We hope this overview paper may contribute as the first step to promotion of regional collaborations in the radar observations and data usages and applications in order to efficiently monitor the coastal and marginal sea waters along the western Pacific Ocean periphery.

Key words – oceanographic radars, monitoring of coastal current and wave, data management and application

1. Introduction

Kuh Kim

Ocean currents are equivalent to the winds in the atmosphere and determine the movement of sea water. For coastal managers, emergency responders, and marine scientists to effectively perform their missions, densely distributed current data that cover larger areas of coastal waters need to be continuously received in a timely manner. However, conventional *in-situ* single-point measurements are insufficient to provide detailed information required by scientists and coastal managers.

Since Barrick et al. (1977) developed the first ground-wave High Frequency (HF, 3~30 MHz) radar, oceanographic radar systems have been developed to provide near real-time two-dimensional maps of oceanic flow over a much larger area out to about 200 km from the shore, resolving spatial scales of about 0.5 to 50 km. Oceanographic radars have been recognized as a cost-effective means to expand the existing system of *in situ* measurements by providing increased spatial and temporal resolution of surface current velocity measurements for important ecological, economic, and safety applications. Presently there are more than 290 global ocean radar stations with 100 long range (3~10 MHz), 168 standard range (10~30 MHz) and 22 VHF (>30 MHz) radars (Fig. 1.1).

The underlying physics of surface current and wave spectra measurements by oceanographic radar is radio wave backscattering from a moving rough sea surface (Bragg scattering, Crombie 1955). First-order Bragg scattering is due to surface gravity waves whose wavelength is half the transmitted HF radio wavelength. The Doppler frequency

*Corresponding author. E-mail: kuhkim@gmail.com

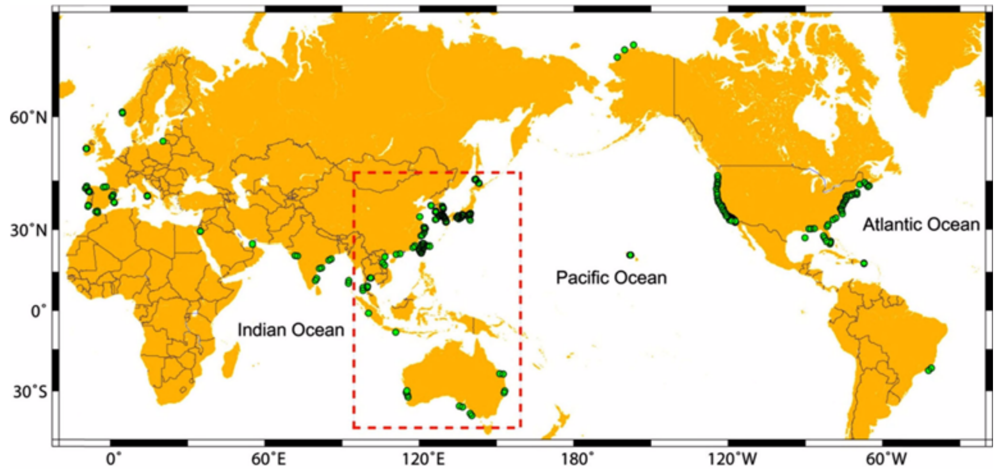

Fig. 1.1. Global ocean radar sites (Source: http://assets.maracoos.org/). Dashed line area denotes the Asia and Oceania countries participating in the 1st Ocean Radar Conference for Asia (ORCA)

shift of the received signal is determined by the phase velocity of scattering waves superposed on the underlying currents. The difference between the measured velocity and theoretical phase velocity of the Bragg waves is attributed to the radial velocity (away from or towards the radar) of the surface current (Barrick et al. 1977). More than two radial velocity components measured from different antenna locations are required to produce the speed and direction of ocean surface current vector. While first-order Bragg scattering yields information on the scattering wave only, second-order scattering data have the information of surface wave energy spectrum (Hasselmann 1971; Barrick 1977).

Presently, oceanographic radar systems are basically categorized in two groups by the azimuth resolving technique. A crossed-loop receive antenna is used by the SeaSonde, CODAR systems using MUSIC algorithm for direction-finding, while phased-array systems are used by WERA and several other national systems. The phased-array genre is further split into Beam-Direction-Finding (BDF), where the beam is formed by hardware, and Digital-Beam-Forming, where the beam is formed in the analysis stage after the data have been collected. The SeaSonde uses pulsed FMICW (Frequency Modulated Interrupted Continuous Wave) modulation with a 50% duty cycle, and the WERA uses continuous FMCW modulation. Visit to CODAR (http://www.codar.com/) and WERA (http://www.helzel.com/de/6035-WERA-Remote-Ocean-Sensing/) websites is recommended for more information of basic radar technology, current and wave mapping.

As Asian countries have been rapidly developing, maritime transportation, fishery activities, harbour constructions and coastal zone usages have increased throughout the coastal and marginal seas along the western Pacific Ocean periphery including East/Japan Sea, Yellow Sea, East and South China Seas, Gulf of Thailand, Andaman Sea. Particularly in recent decades, several countries have recognized the importance of near real-time surface currents measured over large areas for safe navigation, oil spill prediction, search and rescue, marine forecasting and tsunami detection and warning as well as the study of ocean current dynamics (IOOS 2009; Hinata et al. 2011). Demands for near real-time surface current and wave measurement have increased, leading to the development of oceanographic radar networks. At the present time there are 119 oceanographic radar stations operating in Asia and Oceania countries with 41 long range, 69 standard range and 9 VHF radars (Table 1.1, see Figure 1.2 for their location). A few countries have developed their own radar systems and the others have used commercially available radar units.

In this paper we introduce the oceanographic radar networks of Australia, China, Japan, Korea and Taiwan, presented at the 1st Ocean Radar Conference for Asia (ORCA), with an overview of the history and purpose of each country's network development, radar systems (sites) and demonstrated performance, data management, major scientific results and applications, so as to share experiences and information about radar operation and to promote the efficient use of radar-derived data. The next sections are composed by each country's authors and arranged in the alphabetic order of the country's name.

Table 1.1. Oceanograohic radars currently operating in Asia and Oceania countries. CL and PA denote antenna types of crossed-loop and phased-array

Frequency \ Country		Australia		China		Japan		Korea		Taiwan		Indonesia		Thailand		Vietnam		Total No.
		CL	PA	CL	PA	CL	PA	CL	PA	CL	PA	CL	PA	CL	PA	CL	PA	
Long Range <10 MHz		4	6	4	4	2	2	1		11		2		2		3		41
Standard Range	10-16 MHz		2	2	5	8		7						4				28
	24-26 MHz					8	16	13		4								41
Short Range >30 MHz			2			2	1	4										9

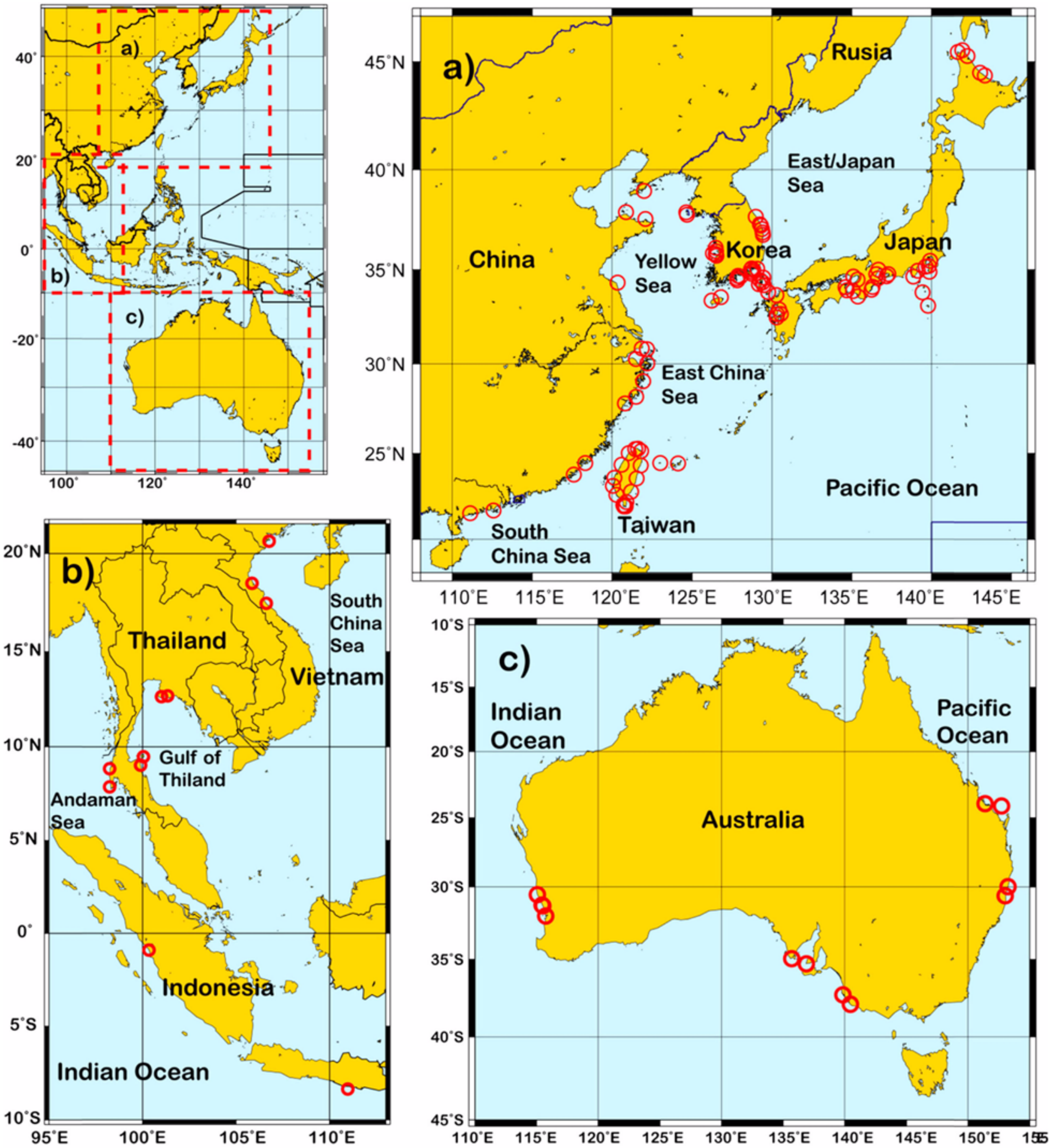

Fig. 1.2. Oceanographic radar stations in Asia and Oceania countries

2. The Australian Coastal Ocean Radar Network

Malcolm L. Heron and Lucy R. Wyatt

Introduction

The first HF ocean radar in Australia was the coastal ocean radar (COSRAD) built at James Cook University in the early 1980s. COSRAD consisted of two stations operating at 30.0 MHz with 50 KHz bandwidths. These were beam-forming phased array systems with 16 elements used for both transmit and receive functions. The beam-forming system used hardware to switch phase shifts to steer the beam into a selected direction to record time series at all the ranges in that direction. The COSRAD system was conventional pulsed A-scan radar which transmitted up to 1000 W in each short pulse. This was a portable system which could be installed in one day and was used for many temporary deployments in Australia to study coastal dynamics and to support engineering projects. (Heron 1985; Heron et al. 1985). The COSRAD system demonstrated the value of HF ocean radar for coastal oceanography and provided the experience needed to meet the challenges of establishing a network of HF radar installations.

The Australian Coastal Ocean Radar Network (ACORN) is part of a National Collaborative Research Infrastructure Strategy (NCRIS) established by the Federal Government to enhance and streamline the funding for research infrastructure across a wide range of areas of science. One area recognised was monitoring of the coastal waters and adjacent deep oceans within the extended economic zone. The Integrated Marine Observing System (IMOS) was established under NCRIS to monitor these waters using appropriate technologies, and deposit fully curated data onto a national data archive which is freely available for research and maritime operations. The IMOS strategy is to support research into coastal dynamics and exchange between the open ocean and the continental shelf. This involves a wide range of facilities including fixed moorings, Argos drifters, ships of opportunity, a fleet of gliders, satellite remote sensing and HF ocean radars.

The establishment period for IMOS was 2007-2011, with many research groups making use of the data archive. Subsequently the goal of IMOS is shifting towards applications in anticipation that some of the facilities will become operational in providing real-time data and forecasts to users. ACORN data in the form of surface current maps are to study ocean dynamics, interactions between physical parameters and ecology, management in the mixing of water bodies and physical connectivity between reefs and islands. Wave and wind data are being added to the archive from the phased-array ACORN radar sites. There is potential for application of the data to marine safety, management of coastal marine resources, resource assessment and operational monitoring for marine renewables, calibration/validations of, and assimilation into, models. With the establishment of HF radar monitoring stations in ACORN and similar networks, there is a growing opportunity for researchers around the world to access data from well curated archives to carry out basic research on physical oceanography, or applied research in coastal zones, as well as to develop data products for maritime agencies and operators.

The establishment of ACORN

ACORN consists of 12 HF radar stations at 6 sites around the southern part of the Australian continent, see Figure 2.1. An early decision was made to include both the phased-array beam-forming and crossed-loop direction-finding technologies with the primary aim of giving future planners some local experience with each of the genres of systems. Of the four sites funded by IMOS directly, two are phased-array and two are crossed-loop; the other two sites were funded independently by agencies who specified the need for wave data, and phased-array systems were chosen. In all cases the primary function of the radars was to map surface currents, and in most cases spatial resolution was sacrificed

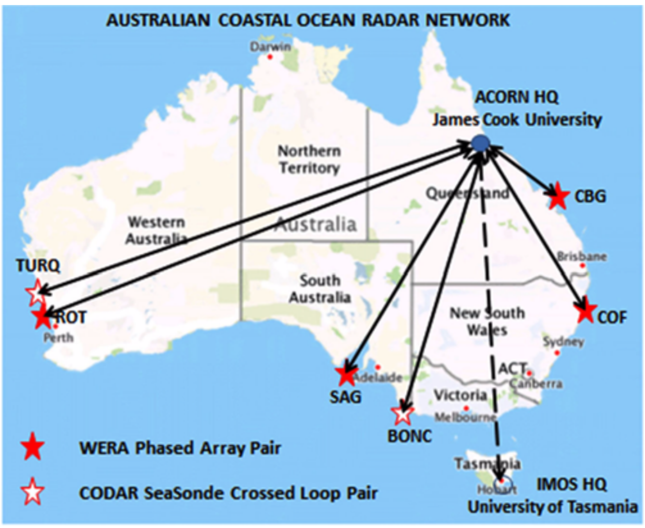

Fig. 2.1. The ACORN network consists of 12 stations at 6 sites shown by the stars

in order to achieve the longest ranges possible. Five of the sites are designed to cover ranges to at least 150 km for surface currents, with the system at Coffs Harbour operating to 120 km (Table 2.1). Where wave data were required, the WERA phased-array systems are being used to give maps of significant wave height to about half the operating range for surface currents, and in a more restricted area to provide directional wave spectra. The network is managed from the ACORN headquarters at James Cook University in Townsville where all data are received, checked for quality, cast into netCDF format with relevant metadata, and sent to the archive under the management of the IMOS headquarters at the University of Tasmania.

The SeaSonde crossed-loop systems were installed under the supervision of the manufacturer, and their recommended configuration and analysis parameters were used, except for the final integration time which was reduced from 180 minutes to 80 minutes in order to capture tidal signals. The SeaSonde systems have spatial resolution of 20-50 km (Heron et al. 2012). The WERA phased-array systems were installed under the supervision of the manufacturer and configuration parameters were agreed. The WERA systems have spatial resolution of 8-25 km (Heron et al. 2012). ACORN developed a new quality control processing for WERA data which is applied to the archived data in a post-analysis method where there is a delay for several months to allow for raw files to be transferred from the stations to the ACORN headquarters.

To meet the wave and wind measurement needs at the WERA sites, ACORN has obtained a specialised software package and this is currently being tested with data from CBG, SAG and COF. This software was developed from the work of Wyatt et al. (2011, 2012) and, where data quality is suitable, this provides estimates of the directional spectrum and derived parameters (e.g. significant wave height) and of wind direction.

The phased-array stations are given 3-character names, and the crossed-loop station names have 4 characters: these names are carried through to the data files in the archive. On the east coast, the Great Barrier Reef, Capricorn/Bunker Group (CBG) and Coffs Harbour (COF) sites are monitoring the East Australian Current (EAC) which is a western boundary current flowing southwards. Capricorn/Bunker Group (CBG) is in the southern part of the Great Barrier Reef where the warm EAC waters impact the shelf, and Coffs Harbour (COF) is where the EAC starts to separate from the coast to form large billows and eddies in the Tasman Sea.

The Bonney Coast (BONC) in South Australia has a seasonal cold upwelling which is being monitored, and the entrance to the South Australian Gulfs (SAG) is a key area for shipping, mariculture and ocean dynamics of the gulfs. The stations in Western Australia monitor the Leeuwin Current on the Turquoise Coast (TURQ) where there is a significant lobster fishery industry and off Rottnest Island (ROT) where there is a deep canyon across the shelf which supports the biggest diversity of species on the west coast.

Highlights and performance

The ACORN network is producing good quality near real-time data for research and applications. Typical quality and coverage are illustrated in Figure 2.2a and 2.2b. These are daytime data: at night the range is compromised on all HF radar systems when the ionosphere does not attenuate noise and interference from distant sources.

One highlight for ACORN during its establishment phase was the opportunity to display the capacity of the phased-array system in the southern Great Barrier Reef (GBR) when the coal carrier Shen Neng I ran aground on Douglas Shoal on 3 April 2010, fully laden with 65,000 tonnes of bulk coal and 975 tonnes of fuel oil. The vessel was under

Table 2.1. The radar sites for ACORN. The site names apply to pairs of stations and are referenced to Figure 2.1. The operating frequencies and bandwidths are allocated by the Australian Communications Management Authority. PA and CL of radar type denote phased-array and crossed-loop

ACORN Site	Radar Type	Operating Frequency (MHz)	Band Width (kHz)	Designed Range for Currents (km)	Wave Data	Time Resolution of data (min)
CBG	PA	8.34	33	150	Hs maps	10
COF	PA	13.92	100	120	Hs maps	10
BONC	CL	5.21	50	150	Hs point	80
SAG	PA	8.34	33	150	Hs maps	10
ROT	PA	8.34	33	150	Hs maps	10
TURQ	CL	5.21	50	150	Hs point	80

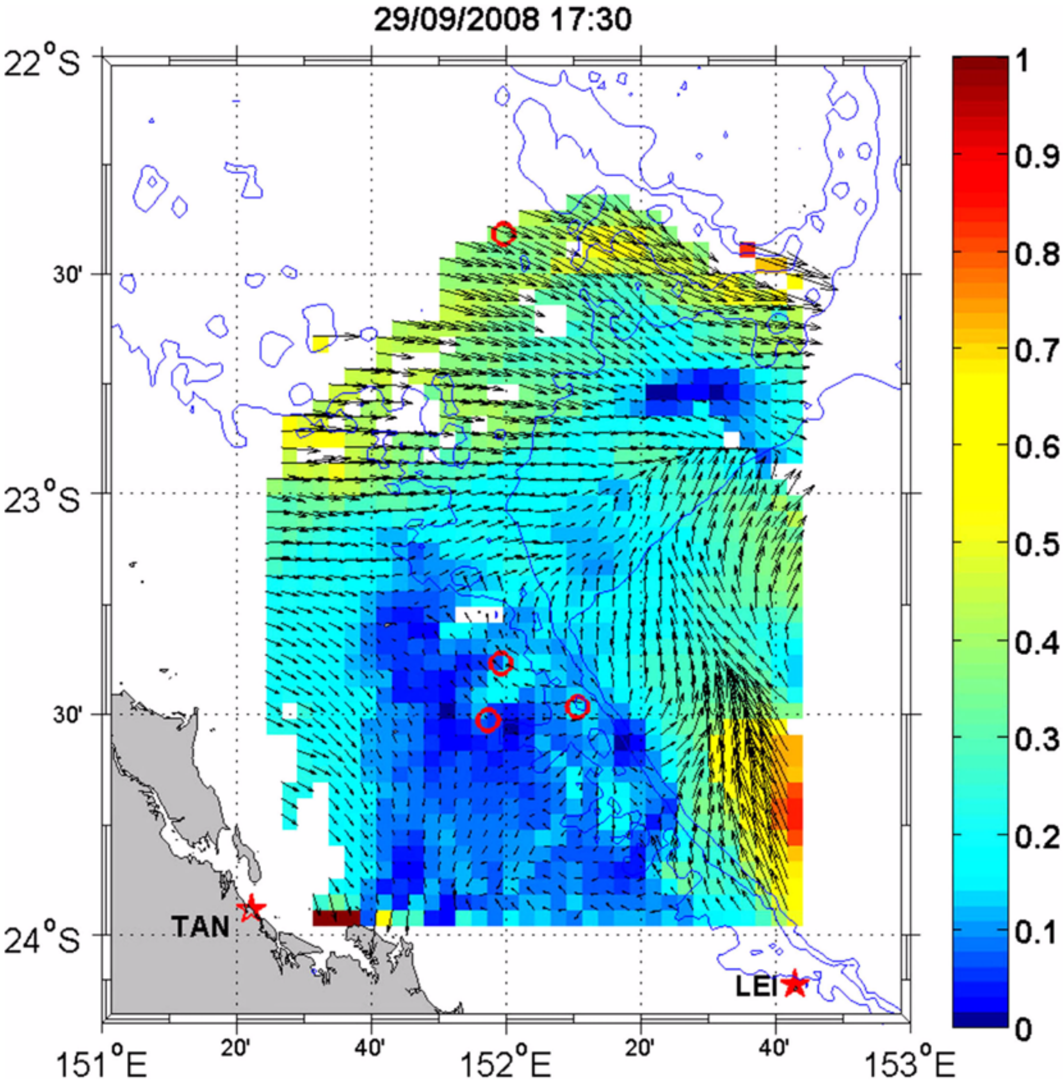

Fig. 2.2a. A typical map of surface currents in the southern part of the Great Barrier Reef (CBG) where a phased-array system is installed at Tannum Sands on the mainland, and Lady Elliot Island on the edge of the continental shelf (red stars). The eastern edge of the line of reefs and islands is the delineation of shallow (40-50 m) water on the continental shelf to the west, and deeper oceanic water to the east. The circles mark the positions of in situ observations for validation. The arrows have length proportional to the currents speed and the direction is that of the current. The colour shading is for visualisation with the colour bar showing speeds in m/s. This map is a 1-hour sample without smoothing

way at full speed when the grounding occurred and she sustained severe damage to her port side, and to the propeller and rudder. The incident occurred at near low tide, and on 12 April she was re-floated with the aid of tugs after all the oil had been removed.

Incident reports indicate that the oil spill was effectively contained and dispersed, with most of the oil being removed from the ship's tanks. The main environmental damage was to the coral ecology by the movement and grinding of the hull on the coral reefs. The visible plume consisted of finely ground calcium carbonate, rather than oil. The site was within the area mapped by the CBG radar and, in post analysis, we created Lagrangian tracks of surface water starting from the site at daily intervals, as shown in Figure 2.3. For days 1 through 4 the surface drift was to the west and south-west (Heron et al. 2010). This was confirmed by the presence of some tar balls in that area. On day 5 the wind turned to come from the south-east and for the next 6 days the surface water was driven to the north-west. With the tracks shown in Figure 2.3 commencing

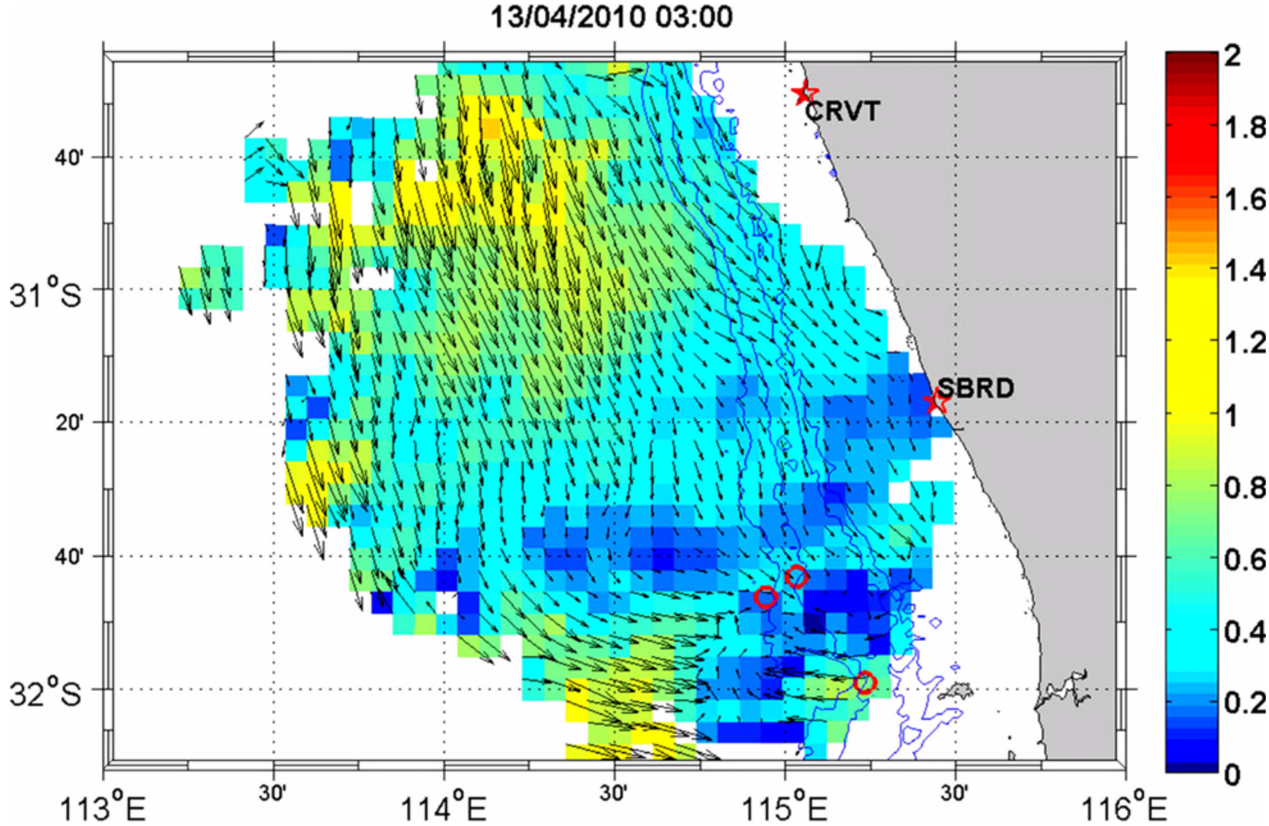

Fig. 2.2b. A typical map of surface currents on the west coast where a crossed-loop system is installed at Cervantes to the north and Seabird in the south (red stars). The dominant flow in the off-shore zone is the southwards Leeuwin Current, with meanders on the shelf. The arrows have length proportional to the currents speed and the direction is that of the current. The colour shading is for visualisation with the speeds shown in the colour bar (m/s). This map is an 80-minute sample with smoothing and gap-filling

daily, it is possible to pinpoint the loci of the tracks at any later time. The solid orange line shows the loci after 11 days and marks the slick line for any flotsam or pollution at that time. This demonstrates the ability of this phased-array system with its good temporal and spatial resolution, to track individual water parcels in the ocean surface.

The data archive

The radial components of surface currents at each radar station are the basic data. For the SeaSondes these radial data are archived hourly in a polar coordinate system. For the WERAs they are archived every 10 minutes on a rectangular grid. Other parameters provided by the manufacturers' software are also included in these files. In the case of WERA this includes an estimate of significant wave height and the first order Bragg energies from which wind directions can be inferred. Radial data from two stations are then used to calculate hourly values of the u, v components of the surface current vectors on a rectangular grid in both cases. In the case of the SeaSondes the standard CODAR software is used, i.e. a least square fit to all data within a 10 km radius around the grid point of interest; in the case of WERAs the same grid is used for radial and vector currents and the method is a straightforward algebraic operation. The WERA data are re-processed in delayed mode with improved quality and coverage (the re-processing achieves better results in noisy situations) and with quality control (QC) flags according to the SeaDataNet standard (refer www.seadatanet.org). The SeaSonde data are processed using proprietary software which removes interference and noise spikes and includes averaging processes which are represented in the data files by standard deviations of the current component estimates. No additional QC has been carried out on these data. The data can be viewed on, and downloaded from, the IMOS data portal found at www.imos.org.

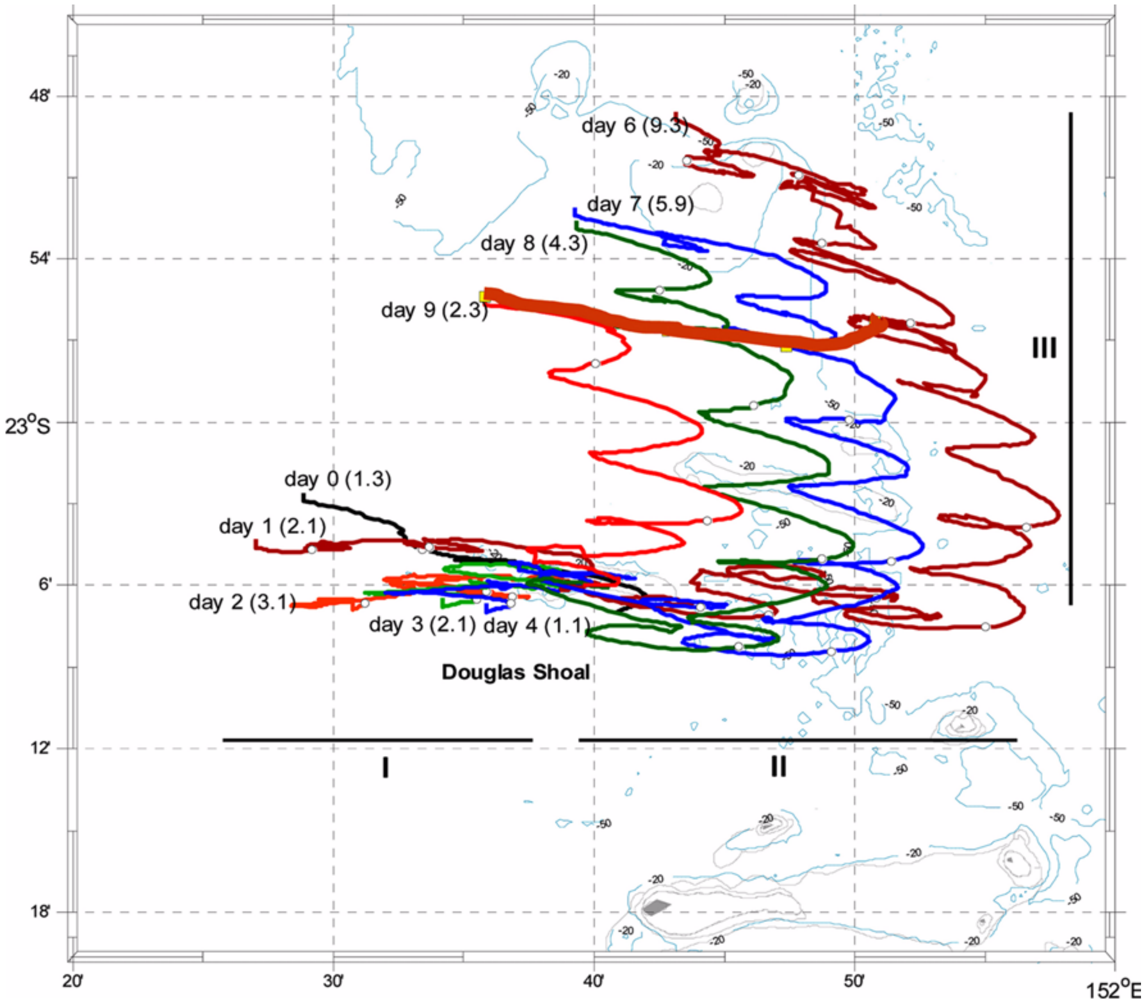

Fig. 2.3. Lagrangian tracking using HF radar data from the CBG phased-array radar system following the grounding of the Shen Neng I in 2010. Tracks were commenced daily following the grounding. The figures in brackets indicate the length of the track in days. The solid orange line joins the positions of the tracked parcels on the 11th day after the grounding

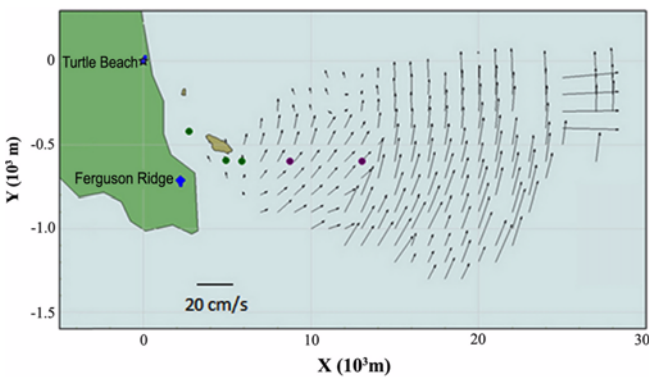

Fig. 2.4. VHF high resolution surface current map at the Australian Institute of Marine Science, Australia. The blue symbols on land are the station locations (location of Turtle Beach station is 19°16.094'S, 147°3.508'E), and the dots mark points of interest for sea water intake pipes. The map shows two distinct bodies of water within the mapped area

VHF ocean radar

In addition to the ACORN radars, a portable VHF radar is being used for mapping currents at very high spatial resolutions in ports and harbours, and coastal sites. The PortMap radar has a frequency allocation of 152.2 MHz with a bandwidth of 1.5 MHz in Australia (and 177 MHz and 6 MHz in USA). It has an operating range of 4 km (at 152.2 MHz) with spatial resolution of the order of 100 m. A typical current map is shown in Fig. 2.4 at the Australian Institute of Marine Science where intake pipes bring salt water ashore for research aquaria. The PortMap radar is finding applications in monitoring the movement of turbid plumes from dredging, planning waste outfalls and turbine sites.

3. The HFSWR Development in China

Xiongbin Wu and Xiangbai Wu

Introduction

China started the HFSWR (High-Frequency Surface Wave Radar) technology studies on sea state surveillance in the 1980s. As the HFSWR has advantages such as all-weather adaptability, large-area surveillance capability and relatively low construction and operation cost, Chinese authorities expect that its application will support and enhance the coverage and efficiency of the coastal administration activities. Several institutes including Harbin Institute of Technology, Wuhan University, East China Normal University and Xidian University, etc., developed different types of HFSWR systems with the support of the National Natural Science Foundation of China, the China National 863 High Technique Project, and some other science and technology projects. Efforts were concentrated on HFSWR system architecture and techniques before the year of 2000 and since then an increasing number of domestic oceanographers have become interested in HFSWR and supported its applications in ocean science study and ocean environment surveillance.

More than 15 HFSWR stations are now operating along the Chinese coastline (Figure 3.1, Table 3.1), including the Ocean State Monitoring and Analyzing Radar (OSMAR) series developed by Wuhan University, the CODAR SeaSonde and the Hezel WERA. Most of them are managed by the State Oceanic Administration (SOA) and the rest by the China Meteorological Administration (CMA). SOA had organized several verification tests on HFSWR's capability of surface dynamics detection since 2000. It has been recognized from the tests that: (1) temporally and spatially stable surface current field (such as tide field) can be

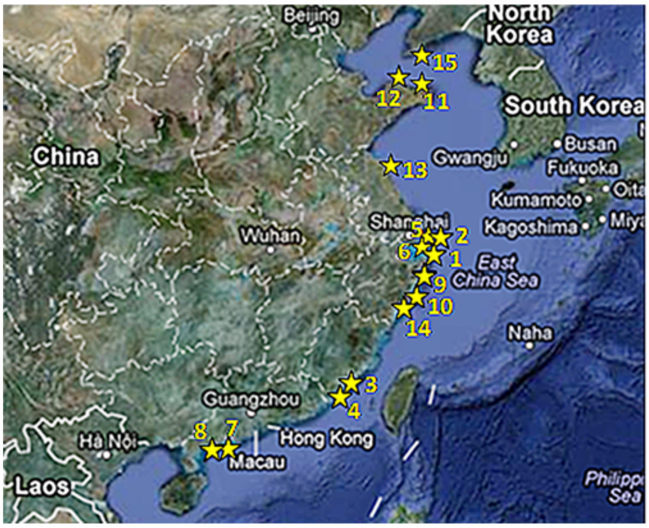

Fig. 3.1. Location of the OSMAR stations marked by the yellow star

Table 3.1. The OSMAR radar stations with the parameters for the operating OSMAR stations in China. See Fig.1 for their locations. The indexes in the table and figure also indicate the construction sequence of the stations. PA and CL of radar type denote phased-array and crossed-loop

Index	Location	Radar Type	Operating Frequency (MHz)	Band Width (kHz)	Designed Range for Currents (km)	Wave Data	Time Resolution (min)
1	Zhujiajian	PA	7.8	30	200	Hs maps	10
2	Shengshan	PA	7.9	30	200	Hs maps	10
3	Longhai	PA	7.9	30	200	Hs maps	10
4	Dongshan	PA	7.9	30	200	Hs maps	10
5	Shengsi	CL	13	60	100	Hs point	20
6	Daishan	CL	13	60	100	Hs point	20
7	Yangjiang-1	PA	13	30	150	Hs maps	10
8	Yangjiang-2	PA	13	30	150	Hs maps	10
9	Shipu	CL	7.5	30	200	Hs point	20
10	Dachen	CL	7.5	30	200	Hs point	20
11	Weihai	CL	7.7	30	200	Hs point	20
12	Penglai	CL	7.7	30	200	Hs point	20
13	Dafeng	PA	13	30	150	Hs map	10
14	Wenling	PA	13	30	150	Hs map	10
15	Dalian	PA	13	30	150	Hs map	10

detected by HFSWR with quite high accuracy and reliability; (2) results from different systems demonstrate different temporal and spatial resolutions; (3) dynamics derived from the second order Doppler spectra of the echoes (such as wave height, wind velocity, etc.) show poor quality and low reliability compared with surface current information which is extracted from the first order peaks; (4) low HF band radar systems, which are designed to cover more than 100 km range, are exposed to intensive natural or artificial radio interferences and noises in the southern China coast areas, thus data were not quality-controlled. The Chinese authorities consider further studies are needed to solve or alleviate the above inversion and interference problems before more HFSWR stations or HFSWR network would be established in the future.

Development of the OSMAR HFSWR technique

The Space Physics Department of Wuhan University developed the OSMAR series HFSWR in the late 1980s, and the first prototype OSMAR was tested on the coast of Guangxi Province in 1993 (Hou et al. 1997). The development of OSMAR was mainly motivated by the early CODAR system of the United States after one of the CODAR technicians gave lectures on HFSWR in Hangzhou, China. Because the Wuhan University has the longest history of HF radio wave propagation study among Chinese universities, it is not surprising that the OSMAR HFSWR studies were carried out right after that lecture. The 1993 system adopted the early CODAR's 4-element square array and the test results showed that the OSMAR had measured the tidal current information of the Beibu Gulf to some extent out to a range of about 15 km.

In 1996, the China National 863 High Technique Project began to support technique studies on oceanic science and engineering and a 200 km-coverage OSMAR proposal was among those supported. In 2000, the OSMAR2000 was completed and a short-term test showed that the radar-measured currents field had similar spatial and temporal variations to in-situ measurement out to 200 km during daytime. The second order echoes could be observed to a range of about 60 km when the sea state was not low. The OSMAR2000 receiver adopted the 7.5 MHz FMICW waveform and three intermediate frequency conversion superheterodyne structure. It had a three-element Yagi transmitting antenna and a receiving array composed of eight linearly-deployed dipole antennas. MUSIC algorithm was applied to extract current information from first order peaks and a software based beam forming method was used to serve for inversion of wave and wind information (Wu Xiongbin et al. 2003).

Industrial OSMAR products were put forward in 2004 as the HFSWR operators require reliable and easy-to-use equipment in their observation activities. These products' design and production process meets the ISO standard requirements. Some new aspects of the latest OSMAR include: (1) automatically calibrating the amplitude and phase mismatching factors between receiving antenna channels by analyzing the statistics of sea echoes; (2) allowing alternatively frequency-changing among FMICW sweeping frames, making multi-frequency detection possible; (3) full digital receiver techniques have been adopted; (4) Client/Server (C/S) type database is applied in software to manage radar data sampling, processing, archiving, and visiting.

In 2005 and 2008, two extensive verification tests were carried out by the First Institute of Oceanography of SOA and the Third Institute of Oceanography of SOA to verify the OSMAR current field detection capability. In the 2008 test, 5 ships were deployed at 10 various range and azimuth cells (two sets of 5 simultaneous in-situ measurements) within the radar beam coverage along the Fujian coast to make in-situ current measurements against radar results. RMS errors of vector current time series between the two kinds of measurements varied from 9.7 cm/s to 18.8 cm/s in magnitude and 10° to 29° in direction at different ship locations, where the 18.8 cm/s and 29° error appeared at the location just on the Taiwan Shoal where water depth varies acutely within a horizontal scope of tens of meters.

Regarding the OSMAR wind and wave detection capability, a six-month long comparison of time series (from Nov. 1st, 2008 to Apr. 30th, 2009) had been made between OSMAR results and in-situ measurements made by the Kinmen buoy of Taiwan Water Resource Agency, which is about 30 km from the Longhai OSMAR radar station. RMS errors of significant wave height, wind direction and wind velocity are 0.39 m, 22° and 2.2 m/s, and correlation coefficients are 0.67, 0.70 and 0.52 respectively (Wu Xiongbin et al. 2012).

Applications

SOA established the first four HFSWR stations in 2002, two 7.5 MHz OSMAR stations on two islands of Zhoushan archipelago and two 25 MHz SeaSonde stations near Shanghai, and another two 7.5 MHz OMSAR stations at Dongshan (refer to Figure 3.2) and Longhai, Fujian Province in 2005. Figure 3.3 demonstrates the OSMAR vector current field

Fig. 3.2. The receiving array of the Dongshan OSMAR station

and wave field results. As HFSWR ocean dynamics data are produced by quite different physical processes than routine oceanic observation data, and with intricate effects from radio interferences, data quality control strategy and method appeared to be pivotal in HFSWR application. The work of data quality control for HFSWR data and feasibility of using these data in oceanographic studies were organized and led by Prof Li Yan in Xiamen University.

Zhu et al. (2007) analyzed the spatial pattern of the amplitude and phase of the M_2 tide component from the post quality-control OSMAR radial data as the preliminary oceanographic verification. The results were consistent with previous investigations and it was concluded that after proper quality control the radial currents from the HFSWR system were capable of being used to monitor the temporal and spatial variation of the surface currents. Long time-series of sea surface current data sets from HF-radar system were used to decompose the surface current in the western part of the Taiwan Strait by Zhu et al. (2008), and it was found that the surface current there contains mainly two parts: the seasonal variation of the along-shore currents induced by the monsoon and an all-year-long persistent background northeast flow of about 10 cm/s. The sea surface current data from HF-Radar were assimilated into a parallel computing 3-D numerical oceanic prediction model in the Taiwan Strait together with other multi-sensor ocean data using 4D Variational Data Assimilation method by Zhang (2009), the errors between predicted and observed data were reduced by as much as 32.4% and thus the prediction was greatly improved. Wu and Li (2012) estimated the bottom drag coefficient from the HF-radar current flow, the drag reduction trend over periodic bathymetry (sand waves) was revealed and a new drag coefficient for a regional numerical model was provided.

As East Asia suffers a lot from typhoons, SOA is interested in the role HFSWR could play during typhoon events. There have been several cases where the OSMAR recorded the processes of typhoons passing across the radar coverage or landing on a coast. Figure 3.4 depicts the eye of the Lion Mountain typhoon at 4:00LT, Sept. 2nd, 2010, during its landing process onto the Fujian coast.

Xiamen University and Wuhan University have also organized experiments to extend HFSWR's application potential. One of these experiments involved exploring the

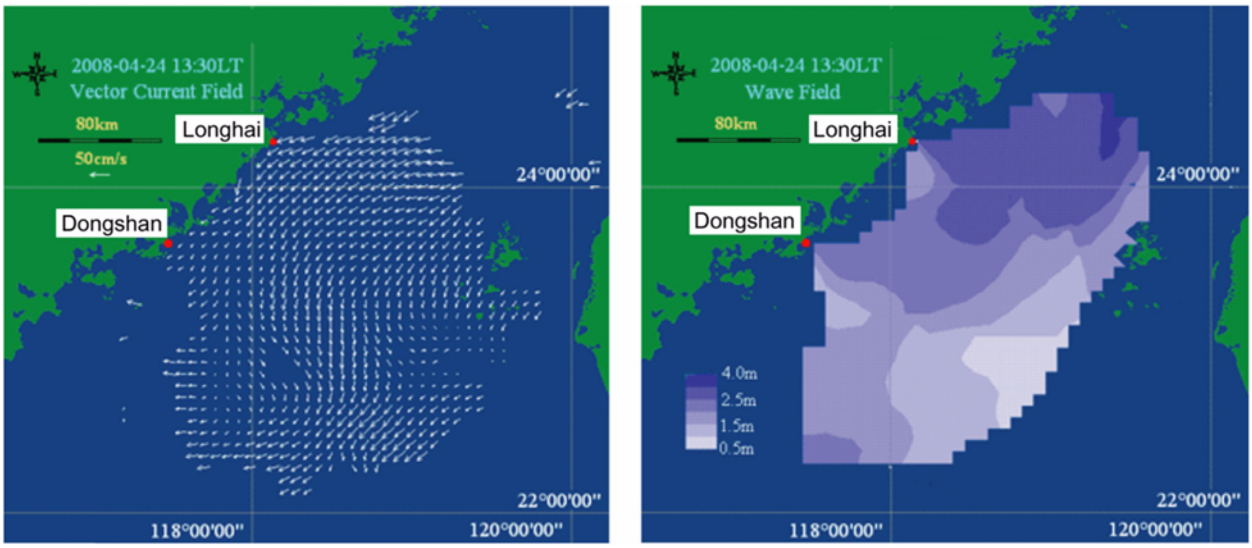

Fig. 3.3. Vector current field (left) and wave height field (right) output from the Longhai and Dongshan OSMAR stations in April 24, 2012

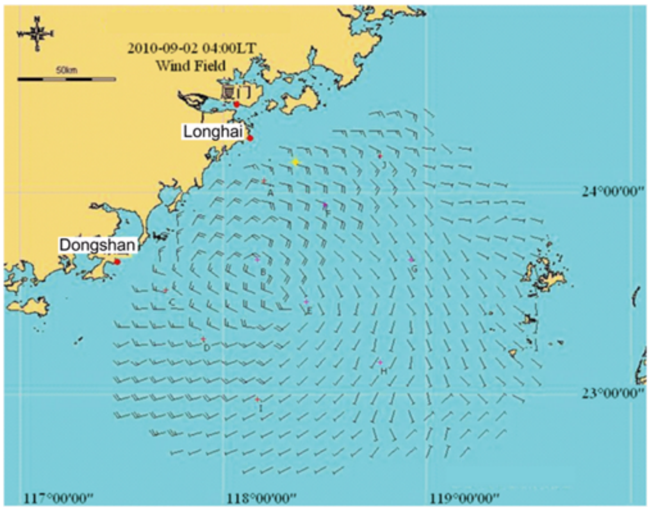

Fig. 3.4. One of the wind direction field mapped by the Dongshan and Longhai OSMAR sites at 04:00LT on Sept. 2nd, 2010 as the Lion Mountain typhoon was approaching the Fujian coast

inversion algorithm for the sea surface's conductivity distribution by calculating the attenuation factor of HFSWR radio waves along its propagation path. Another experiment (attended also by Nanjing University) was done during the summer of 2011 in the offshore shoal region of the north Jiangsu coast, where water depth is about several meters to more than 10 meters, and three temporary HFSWR sites were setup to "measure" the water depths by figuring out the Bragg wave's phase velocity variations from its deep water value. Strong non-linear interactions between current, wave and floor were observed and they created some interesting characteristics in the spectra of the echoes. Studies on them are on-going.

Future work

China is trying to promote HFSWR's development by balancing relationships between radar techniques, application methods and requests resulting from state maritime activities. Studies on HF radar networking techniques and on a practical indices system for evaluating HFSWR's performances will be supported under a new round of the 863 Project from 2012 to 2015. More and more Chinese oceanographers are showing interest in HFSWR application in their research, and efforts are being undertaken to establish a national-wide HFSWR network that will benefit both scientific study and oceanic environment surveillance.

4. Oceanographic Radar in Japan

Satoshi Fujii

Introduction

In the 1970s and early 1980s feasibility studies for oceanographic radar were carried out by the Meteorological Agency and the Maritime Safety Agency (currently the Japan Coast Guard: JCG) in Japan. Also the Radio Research Laboratory (later Communications Research Laboratory: CRL, and currently the National Institute of Information and Communications Technology: NICT) made preliminary research with the use of LORAN-A signals. However, none proceeded to make a deployable oceanographic radar.

In 1986, the Okinawa Radio Observatory of Radio Research Laboratory (currently the Okinawa Electromagnetic Technology Center of NICT) began to develop oceanographic radar by modifying a microprocessor-controlled ionosonde. This radar used a phased array system as both transmit and receive antennas with steering beams produced by an electronics switch phase-shifters. The first observation of the Bragg peaks from ocean waves was made in October 1988.

After two decades, about 50 radars using several frequency bands have been installed and are operated for research and monitoring of coastal areas in Japan.

Radar system and site

All radar systems in Japan use pulsed and gated FMCW (Frequency Modulated Continuous Wave), which is also called FMICW ("I" means "interrupted"), waveforms with collocated transmit and receive antennas. The five frequency bands within 3-50 MHz are allowed for oceanographic radar use in Japan.

Exactly 49 radars are operated with valid licenses as of Oct. 1, 2012. Ten of them are mobile systems for temporal observations and the others are installed at fixed observation sites for continuous monitoring. All oceanographic radars in Japan are shown in Figure 4.1.

Frequency and bandwidth

Higher frequency radar has a shorter observation range, because the higher frequency causes more attenuation in ground wave propagation. The bandwidths that determine the range resolution are decided for each of the frequency bands.

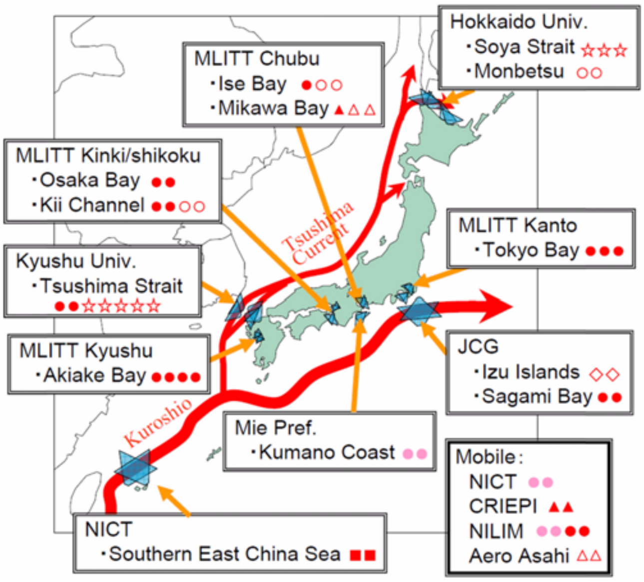

Fig. 4.1. The number of symbols indicates the number of oceanographic radars installed in Japan. The shape of a symbol indicates the frequency of a radar; ◇ 5.0 MHz, ■ 9.2 MHz, ☆ 13.9 MHz, ● 24.5 MHz, ▲ 41.9 MHz. The Solid symbol is for the phased-array DBF system, the dark symbol for the phased-array beam steering system, and the open symbol for the SeaSonde crossed-loop system

Four frequency bands in the HF-band (3-30 MHz) and one in the VHF-band (30-300 MHz) are permitted for oceanographic radars in Japan. Almost all radars are licensed as experimental usage world-wide because there was no allocation in HF bands for radio location service (which is the official term for radar) in the radio frequency administration rules of ITU-R (Radiocommunication Sector of International Telecommunications Union) prior to 2012.

- 5.0 MHz: For long-range operation, lower HF frequency band achieves a range of 200 km or more. The range resolution of 10 km is made by the bandwidth of 15 kHz. Two radars are operated by JCG in the Izu Islands area.
- 9.2 MHz: For long-range operation, this band achieves a range of 200 km or more, similar to the 5.0 MHz band. The range resolution of 7 km is made by the bandwidth of 22 kHz. Two radars are operated by NICT at the southern part of the East China Sea.
- 13.9 MHz: For middle-range operation, observation distance reaches 70 km in the best propagation condition for current measurements. This band has a bandwidth of 50 kHz that makes for a range resolution of 3 km. 8 radars are operated; 3 radars by Hokkaido University at Soya Strait; 5 radars by Kyushu University at Tsushima Strait.
- 24.5 MHz: Approximately 60% of radars in Japan use this band, which achieves about a 50 km range for littoral-area monitoring. This band has a bandwidth of 100 kHz that makes for a range resolution of 1.5 km. 24 radars are installed at 9 observation sites over Japan, 6 of which are operated for mobile use for temporal observations.
- 41.9 MHz: This frequency band is the only one in the VHF-band and is convenient for environmental monitoring in estuary areas within 30 km from the coast with a high resolution of 500 m using a bandwidth of 300 kHz.

Radar system

29 radars of the 49 radars are SeaSonde/CODAR crossed-loop direction-finding systems. These radars are operated with monopole or 3-element Yagi antenna transmitting 40-50 W averaged power except for 25 W transmit power of the 41.9 MHz band radar for short-range observations.

The other 29 radars are phased-array beam-forming systems. These phased-array radars have 100-200 W transmit power which is used for short-time observations of 10-20 minutes duration. A typical phased-array is composed of from 6 to 10 antennas as monopole with reflector (2-element Yagi) or 3-element Yagi antenna. There are two types of phased-array system in Japan. The older systems are beam-steering made by a beam-forming network with electronically controlled phase-shifter. Both receiver and transmitter use the same antenna system with switching alternately. The newer systems use different antennas for receiver and transmitter. In the newer one, the phased-array is the receiving antenna, and the antenna elements are followed by individual receivers. Observation beams are composed mathematically after digitizing the received signals. This type of method is called Digital Beam Forming (DBF). 23 radars belong to the phased-array DBF system and the 6 others belong to the phased-array beam-steering system.

The radar systems for temporal observational use are described as follows and those in the fixed observation sites are described in the next sub-section;

NICT 24.5 MHz radar: The first NICT radar was the first oceanographic radar in Japan mentioned above. NICT continued to develop some other original types of radar and the last 2 phased-array beam-steering radars are still being maintained. These can steer the beam in 13 directions for transmit and receive with 10 monopole-antennas each with a reflector element. More than 20 temporary deployments were performed over Japan using these NICT radars involving many institutes for basic studies and application of oceanographic radar during the early years of HFSWR in Japan.

CPIEPI 41.9 MHz DBF radar: The Central Research Institute of Electrical Power Industry (CPIEPI) was among the second group of owners of oceanographic radar in Japan. CPIEPI developed two high-resolution radars as result of cooperative research with NICT. These radars are made by Mitsubishi Electric Corporation (MELCO) and operated in the 41.9 MHz band with phased-array DBF technology using eight 3-element Yagi antennas. This system is for environmental research in estuary areas and for tracking warm water discharge from power plants using the high spatial resolution capability of 500 m with short-time interval of less than15 minutes.

NILIM 24.5 MHz radar: The National Institute for Land and Infrastructure Management (NILIM) of the Ministry of Land, Infrastructure, Transport and Tourism (MLIT) has 4 phased-array radars: 2 beam-steering and 2 DBF that all are made by Nagano Japan Radio Corporation (NJRC). This DBF radar is the original model of the phased-array DBF radars operated by MLIT in several bay areas. Recently the application for prediction and tracking of drifting objects for garbage collection were researched using these radars.

Aero Asahi's SeaSonde: Aero Asahi Corporation is the representative of CODAR in Japan, and also owns two 41.9 MHz SeaSondes which provide commercial measurement services of ocean conditions. Aero Asahi has performed more than 10 temporary deployments.

Kokusai Kogyo Sea Watcher system: Kokusai Kogyo Corporation is now developing data management and processing parts of the oceanographic radars network and participates in all networks operated by MLIT. Kokusai Kogyo formerly had developed and owned unique radars called Sea Watcher after the cooperative research application with NICT. Sea Watcher was operated at 41.9 MHz band and scanned the beam by mechanically rotating the stacked four 5-element Yagi antennas for both receiver and transmitter. Sea Watcher was used for commercial measurement services until the early 2000s.

Observation site and network

39 radars are installed at 13 observation sites, see Figure 4.1. Each observation network is composed of from 2 to 7 radars and is operated by an individual organization. The data of each network is also gathered and archived individually to each server. Several organizations produce current and wave height maps via the Internet. Unfortunately, at the present time there is no system to manage and integrate the oceanographic radar data on a nation-wide basis in Japan.

Soya Strait: The Soya Strait lies between Hokkaido and Sakhalin, Russia: the northern boundary of Japan. The Institute of Low Temperature Science (ILTS) of Hokkaido University operates 3 SeaSonde systems using the 13.9 MHz band. The radars are networked to the headquarters of ILTS at Sapporo and the data are transferred and processed to make current maps every hour. The Tsushima current flows into the Sea of Okhotsk through the Soya Strait as the Soya warm current (SWC) shown in Figure 4.2(a).

Omu-Monbetsu Coast: The ILTS operates 2 SeaSonde systems using 24.5 MHz band at the northeast coast of Hokkaido on the Sea of Okhotsk. These radars are also connected to the headquarters of ILTS in the same way as the Soya Strait radars. We can find the southeastward current along the coast which is captured as an extension of the SWC.

Tokyo Bay: The Kanto Regional Bureau of MLIT operates 3 phased-array DBF radars with eight 3-element Yagi antennas made by NJRC. These radars are operated at 24.5 MHz with 100 W average powers. The hourly current maps are presented via the web site of the Tokyo Bay Environmental Information Center.

Izu Islands: The Hydrographic and Oceanographic Department of JCG installed 2 long-range SeaSonde systems at Hachijo Island and Nojimazaki at the southernmost tip of Boso Peninsula. These use the 5.0 MHz band to cover a large observation area (200 km × 150 km) around Izu islands. The current maps are calculated every 3 hours. These sites are aimed at monitoring the Kuroshio Current, but there are some difficulties: distorted antenna patterns made by lighthouses nearby and estimated azimuthal velocities in the base line area.

Sagami Bay: The Hydrographic and Oceanographic Department of JCG is operating the other 2 phased-array DBF radars at Izu Oshima Island and Arasaki on the Miura Peninsula to monitor the inner part of Sagami Bay. These are made by NJRC using the 24.5 MHz band with 100 W averaged transmit power, and the phased-array DBF receiver is composed of six 3-element Yagi antennas. Complex currents are observed in this area when a branch of Kuroshio Current is introduced into this area. The hourly current and wave height maps are presented with those of Izu Islands at the web site of JCG.

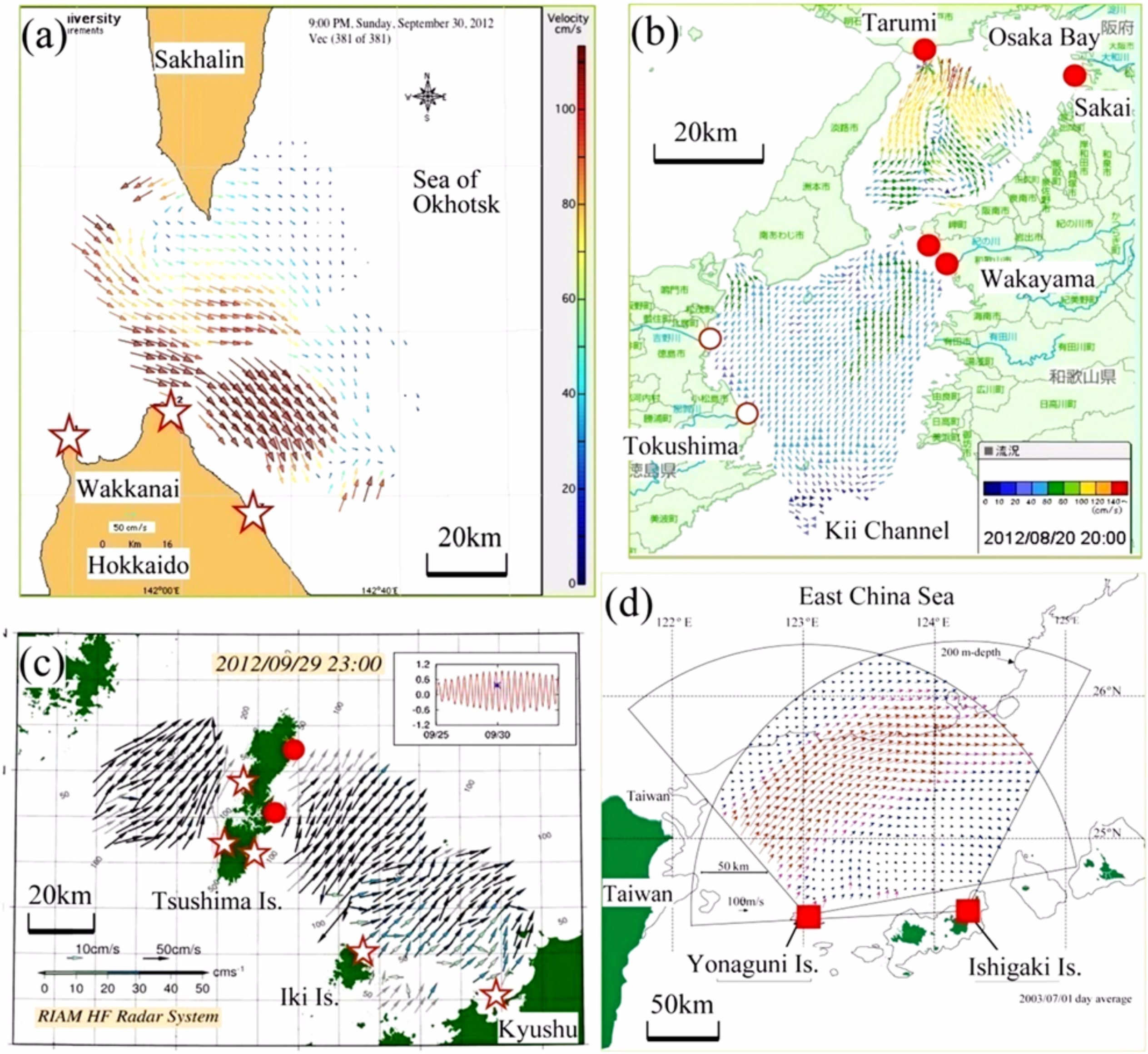

Fig. 4.2. The examples maps of surface currents in the observation area of (a) Soya Strait, (b) Osaka Bay and Kii Channel, (c) Tsushima Strait, and (d) Southern East China Sea. The shape and colour of symbols are the same as in Figure 1

Ise Bay: The Chubu Regional Bureau of MLIT operates and combines different types of radar at Ise Bay. All 3 radars use the 24.5 MHz band; 2 radars are SeaSonde systems and the other one is an NJRC phased-array DBF system with eight 3-element Yagi arrays. Ise Bay is one of the large enclosed coastal seas in central Japan. Continuous environmental monitoring over the bay is performed by hourly mapping and data are archived into the Ise Environmental Database.

Mikawa Bay: The Chubu Regional Bureau of MLIT also operates the same combination of radars using the 41.9 MHz band at Mikawa Bay connected with Ise Bay. Environmental monitoring is more necessary because of concern about pollution of the shallow and small enclosed waters of the bay. These radars are networked with the radars of Ise Bay and the current maps with 500 m mesh are provided and also archived in the Ise Environmental Database.

Kumano Coast: The Mie Prefecture installed two 24.5 MHz phased-array beam-steering radars at Kumano district. These radars which comprise eight 3-element Yagi antennas are made by NJRC. This system mainly aims at measuring wave height for prefectural closed use.

Osaka Bay: The Kinki Regional Bureau of MLIT operates two 24.5 MHz phased-array DBF radars made by NJRC for environmental monitoring of Osaka Bay. These radars are typical NJRC DBF radars comprising eight 3-element Yagi arrays and are installed at Tarumi and Sakai. The data are transferred to the Kobe station to provide current and wave-height hourly maps.

Kii Channel: For monitoring over the Kii Channel which connects Osaka Bay and the Pacific Ocean, on the east side of the channel, two NJRC phased-array DBF radars are installed by the Kinki Regional Bureau of MLIT at Wakayama; on the west side, two SeaSondes by the Shikoku Regional Bureau are installed at Tokushima. All radars use the same 24.5 MHz band. Each system gets interference from other systems because of facing locations. To avoid interference, SeaSonde systems stop continuous transmission for a period of 20 minutes each hour when NJRC Radars transmit, for hourly sampling. The data of all radars are transferred to the Kobe station the same as Osaka Bay data, and the current and wave-height maps of Kii Channel are made every hour as shown in Figure 4.2(b).

Ariake Sea: The Environmental monitoring of the Ariake Sea (which is the largest bay in Kyushu and where extreme tides exceed 4 m), is operated with four 24.5 MHz NJRC phased-array DBF radars by the Kyushu Regional Bureau of MLIT. The four radars are installed around the Ariake Sea and observe the entire sea.

Tsushima Strait: The Research Institute for Applied Mechanics (RIAM) of Kyushu University installed 7 radars network to monitor the Tsushima current which flows through this strait area. Five radars are 13.9 MHz SeaSonde systems and two are 24.5 MHz NJRC phased-array DBF radars. Two SeaSondes are located at the west coast of Tsushima Islands for monitoring the west channel. The east channel is monitored by 5 radars; two NJRC radars and three SeaSondes are located on the east coast of the Tsushima Islands, Iki Island, and Shikanoshima, respectively. These 7 radars are networked to the headquarters of RIAM and hourly current maps like Figure 4.2(c) are produced.

Southern East China Sea: The Okinawa Electromagnetic Technology Center of NICT deployed two 9 MHz long-range radars at the southernmost Japanese Islands, Yonaguni and Ishigaki. These radars are operated with 1 kW transmit power through a 3-element Yagi antenna for experimental use and it has sixteen 2-element Yagi antennas in a line 250 m long for receivers. Observation distance often exceeds 200 km and it can make current maps covering a large area as shown in Figure 4.2(d) including the whole of the Kuroshio stream.

Major results

Introduction of radar systems are published by Ohno (1991), Sakai et al. (2003) and Fujii et al. (2003). For measurement error of current velocity, Nadai (1999) analyzed error distributions in combined total velocities and Yoshikawa (2006) examined errors by comparing with ADCP and between facing radars.

A large number of observation results are reported. For examples of temporary deployments, Kuroshio-water intrusion (called Kyucho) in Bungo channel is reported by Takeoka et al. (1995): in Sagami Bay by Hinata et al. (2005). On the other hand, by using together with the data of fixed continuous long-term observations, Ebuchi et al. (2006) and Yoshikawa et al. (2010) reported on the characteristics of the Soya and Tsushima warm currents respectively. Because the Kuroshio current, which flows along Japan Islands, is the main focus of the long-range radars, many reports about variations of the Kuroshio current are published; for example, Ramp et al. (2008) using JCG radar; Takahashi et al. (2009) using NICT radar. Furthermore, Ichikawa et al. (2008) made comparisons with satellite altimeter data, and Morimoto et al. (2009) discussed current axis variation affected by the strong winds of typhoons.

The methods for calculating the derivation of wave information from oceanographic radar are developed by Hisaki (1996) with a nonlinear inversion of the integral equation and Hashimoto et al. (2003) using a Bayesian method. They are continuing this research to obtain a more efficient and robust method.

Tsunami detection is an important application of oceanographic radars that can give early warnings when the tsunami is still far offshore. The numerical experiments for tsunami detection were first introduced by Fujii and Tokuda (1996). Nevertheless, until March 2011, no-one had observed the signal to confirm the ability to detect tsunami. Hinata et al. (2011) reported the first experience of tsunami detection at Kii Channel at a range of about 1000km from the epicenter of the Tohoku earthquake on March 11, 2011, shown in Figure 4.3.

The textbook of oceanographic radar, "Coastal ocean observation by land-based radar" written by Japanese researchers, was published by the Japan Society of Civil Engineering in 2001. The workshop in which all concerned Japanese parties come together and discuss everything about

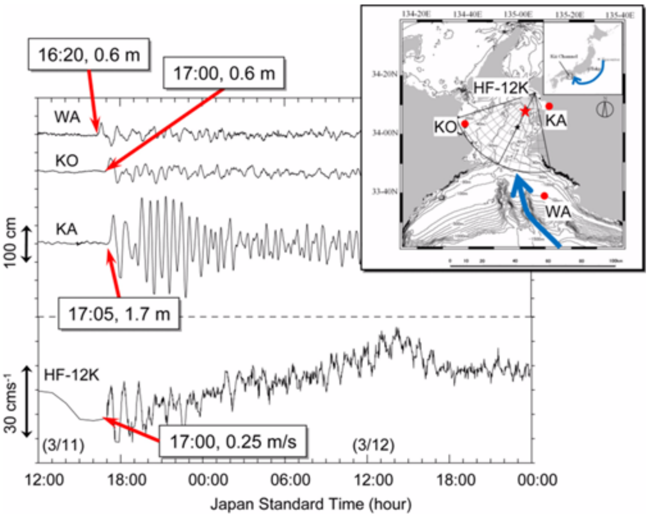

Fig. 4.3. The upper 3 lines are sea surface heights measured at WA, KO, and KA by Global Positioning System, seabed wave gauge, and tide gauge, respectively. The lowest line is a radial velocity at 12 km offshore from radar. These were measured in the period from March 11 to March 12, 2011. The first tsunami wave reached 12 km offshore, 5 min before the arrival of the shore (Hinata et al. 2011)

oceanographic radar is held annually at RIAM, Fukuoka. These are also other types of activities related to oceanographic radar that are conducted in Japan.

The frequency management issue is important globally as well as in scientific research. We proposed new frequency allocations for oceanographic radar collaboration with the U.S. at the WRC (World Radiocommunication Conference) of ITU-R held in 2007. After that, we continued discussions for 4 years in the Working Party 5B, dealing with the radiolocation services in ITU-R, and negotiations with administrative sectors of other countries. The allocation of 10 frequency bands between 3-50MHz was resolved and agreed upon with world-wide approval in the latest WRC-12, February 2012 (ITU 2012). This process has been made possible thanks to good cooperation between the Ministry of Internal Affairs and Communications (MIC) and MLIT. Now we are discussing domestic regulations and guidelines of radio facilities for oceanographic radar in order to maintain consistency between neighbouring counties.

5. Oceanographic Radar in Korea

Sang-Ho Lee and Kuh Kim

Background and history

South Korea is surrounded by the Yellow Sea (YS), the East /Japan Sea (EJS), the East China Sea (ECS) and Korea Strait (KS) (Figure 1.2a). The YS is a semi-enclosed, shallow sea with a mean depth of 45 m, characterized by a large tidal range (4~8 m) and strong tidal currents off the west coast of Korea (Choi, 1980). The ECS and KS is a shelf sea where the Tsushima Warm Current (TWC) passes into the EJS and YS. The EJS has basins deeper than 3000 meters in which strong boundary currents such as East Korean Warm Current (EKWC) and North Korean Cold Current (NKCC) with active eddies are found (Kim et al. 2001).

Measurement of the surface current by oceanographic radar around Korea was first introduced in 1992 when SeaSonde units (CODAR, 25 MHz) were used for demonstration purposes near the Keum River estuary (KRE) on the west coast (Figure 5.1). Since then radar sites have been expanded gradually and currently 25 local radar systems are in operation at regional 8 sites (Table 5.1).

In 2002, Kunsan National University (KNU) installed ocean radars (CODAR, 25 MHz) to map surface currents around the mouth of the Keum River (KRE site). The radar coverage was expanded later in cooperation with the Korea Institute of Ocean Science and Technology (KIOST, its old name was Korea Research and Development Institute, KORDI) on completion of the Seamangeum Dyke, the longest (33 km) in the world, to measure the currents outside of the Dyke. The radar network in this area produced data to examine the effects of large coastal development on the current structure and the extension and variation of river plumes (Lee et al. 2003; Kim et al. 2006, 2008; Son et al. 2007), and the observation-based information of current variability for the effective management and utilization of this coastal area in future.

Korea Hydrographic and Oceanographic Administration (KHOA) has been interested in operational application of ocean radar currents, providing real-time data to the public and a wide variety of end-users (You et al. 2012). KHOA installed radars near Incheon port in 2002 and then moved them in 2003 to Yeosu Bay (YB site) where ship traffic is heavy due to the location of a major harbor nearby, Kwangyang. KHOA added new radar sites at Busan New Port (BNP site) as big container terminals opened recently and to monitor TWC in the western channel of KS in 2011. KHOA also installed ocean radars in 2012 to provide a near real-time surface current field near Baekryeong Island (BRI site) in the YS to assist with military operations. KHOA has a plan to reinstall ocean radars in 2013 on the western coast of Taean County south of Incheon where oil tanker traffic is very heavy.

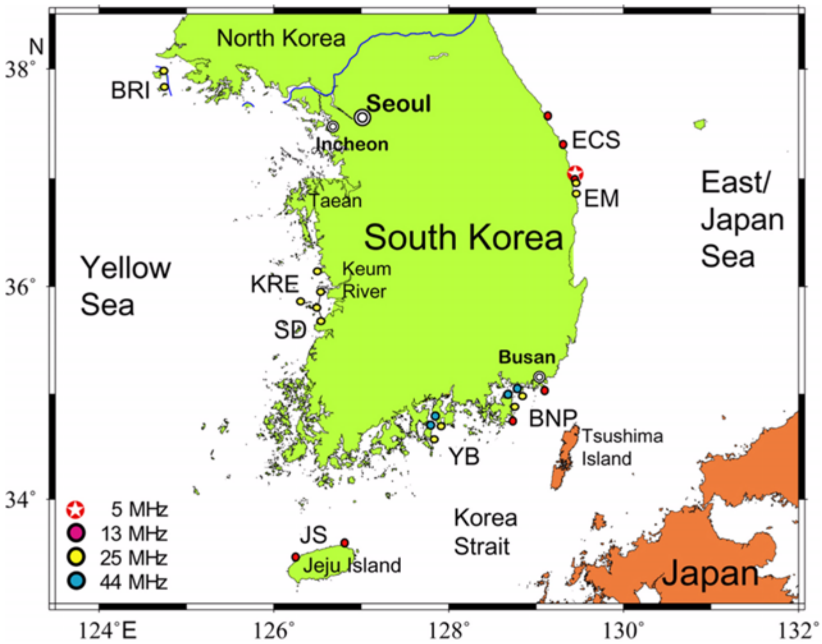

Fig. 5.1. Ocean radar sites in Korea. See the text for the abbreviation indicating site name

Table 5.1. Ocean radar sites in Korea. See Figure 5.1 for site locations. All radars except for 2 radars in the EM site of MIT are CODAR SeaSonde using the crossed-loop antenna

Owner	Site	Number of Radars	Operating Frequency (MHz)	Band width (kHz)	Designed Range (km)	Data Interval (min)	Main purpose
KHOA	YB	2	44	300	15	30	Operational for shipping & navigational safety
		2	25	200	30	30	
	BNP	2	44	500	9	60	Operational for shipping & navigational safety
		2	25	150	30	60	
		2	13	50	90	60	Monitoring of TWC
	BRI	2	25	150	30	60	Operational for navy
KNU & KIOST	KRE	3	25	100	45	60	Monitoring of current by plumes from river and dyke sluices
	SD	2	25	100	45	60	
KIOST	JS	2	13	50	90	60	Jeju warm current monitoring
SNU	ECS	3	13	50	90	60	EKWC & NKCC mapping
		1	5	30	150	60	Frequency and operation test
MIT	EM	2	25	150	50	30	Current and wave mapping

KIOST introduced two ocean radars (CODAR, 13 MHz) in 2012 to observe the current structure and variability in the Jeju Strait (JS site) where the Jeju Warm Current, a branch of TWC, passes to the east through the southern part of Jeju Straits (Song et al. 2012).

Seoul National University (SNU) took over three radars of Bukyeong National University in 2007 after changing their frequency from 25 to 13 MHz to map surface current along the east coast of Korea (ECS site) where the EKWC and NKCC meet and frequently produce complicated current patterns (Son et al. 2012). SNU also tested one long-range (CODAR, 5 MHz) radar successfully in this area and will extend observation coverage by adding a long-range radar in early 2013.

Marine Information Technology Co. (MIT) own two WERA units (25 MHz) with phased array-type antenna of 8 channels and has tested its applicability in current and wave mapping off the east coast of Korea (EM site) since March 2012 (Choi et al. 2012).

In November 2011, Korea Ocean Radar Forum (KORF, http://korf.kunsan.ac.kr/xe/) was formed to share experiences on HF radar network planning, operation, maintenance and data production, and to discuss issues that are common to all operators and end-users in Korea. KORF will hold a workshop every year and aims to establish a national ocean radar network system covering all coastal seas of Korea.

Network maintenance and data management

As local networks in Korea are separated farther than 80 km from each other and most of the radars have standard range frequencies of 13 and 25 MHz, there is no problem of radar frequency sharing and signal interference between local networks at the present time. Korean Electronics and Telecommunications Research Institute checked the environment of ocean radar frequency radio waves along coastal regions of Korea to help radar site hunting and to prepare for WRC's frequency allocation meeting in 2012 (Lee et al. 2012). However, in the future radio transmission frequency sharing will be required for the introduction of long-range radars using highly accurate transmit and receive timing based on GPS time code synchronization (Barrick et al. 2001).

Each network in Korea gathers and archives data individually, and the current maps are provided in near real-time by KHOA (http://www.khoa.go.kr/koofs/kor/observation/obs_real_map.asp) and KNU (http://korf.kunsan.ac.kr/xe/index.php?mid=KNU). The QA/QC procedure is firstly applied to radial and total velocities for each network and the error estimation and gap filling procedure has been already developed (Lee et al. 2008; Hwang et al. 2011; Kim et al. 2012).

The Korean ocean radar community is developing new research and application programs for search and rescue (S&R), ship tracking, tsunami detection and warning, and operational circulation model with data assimilation, with benchmarking of the US surface current mapping plan (IOOS 2009). KORF has a plan to make a standard QA/QC program for the establishment of a nationwide network. KORF also promotes an extension of ocean radar observation coverage to include the exclusive economic zone in order to manage marine resources, conduct ocean dynamic studies, and improve a numerical model by calibration and data assimilation. The upcoming mission of KORF is to cultivate the ocean radar technician community because engineers and technicians will serve as the first responders to a radar site for any disruption of data flow as well as for regular inspection of radar sites for maintenance and calibration purposes.

Major results and applications

Lee et al. (2003) found ebb-jet currents flowing out from the opening of the Samangeum Dyke off the western coast of Korea for the first time by utilizing ocean radar-derived data. Kim et al. (2006) and Son et al. (2007) analysed the M2-tidal current ellipse off the KRE mouth and showed that the major axis direction and phase of net motion were changed by as much as 10~40° counter-clockwise and 30° (~1 hr) due to construction of the northern Saemangeum Dyke (Figure 5.2). Son et al. (2007) also showed that the subtidal currents from HF radar data taken in July 2002

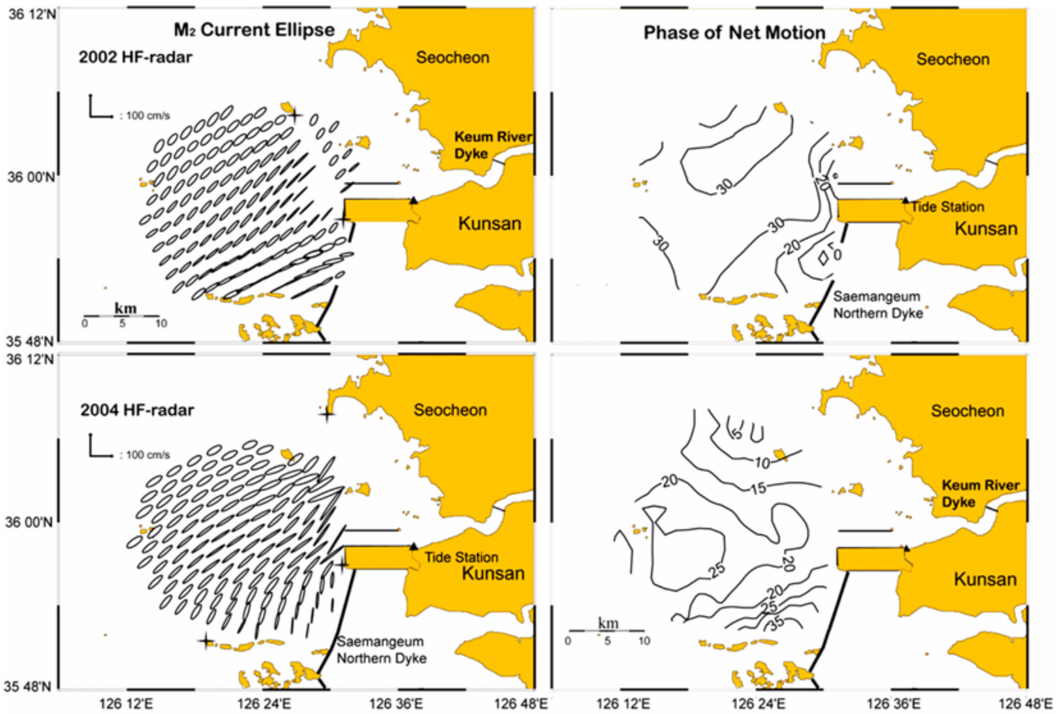

Fig. 5.2. Distributions of tidal current ellipse and net motion phase (degree) of the M2 off the Keum River mouth in July 2002 and October 2004 (after Kim et al. 2006)

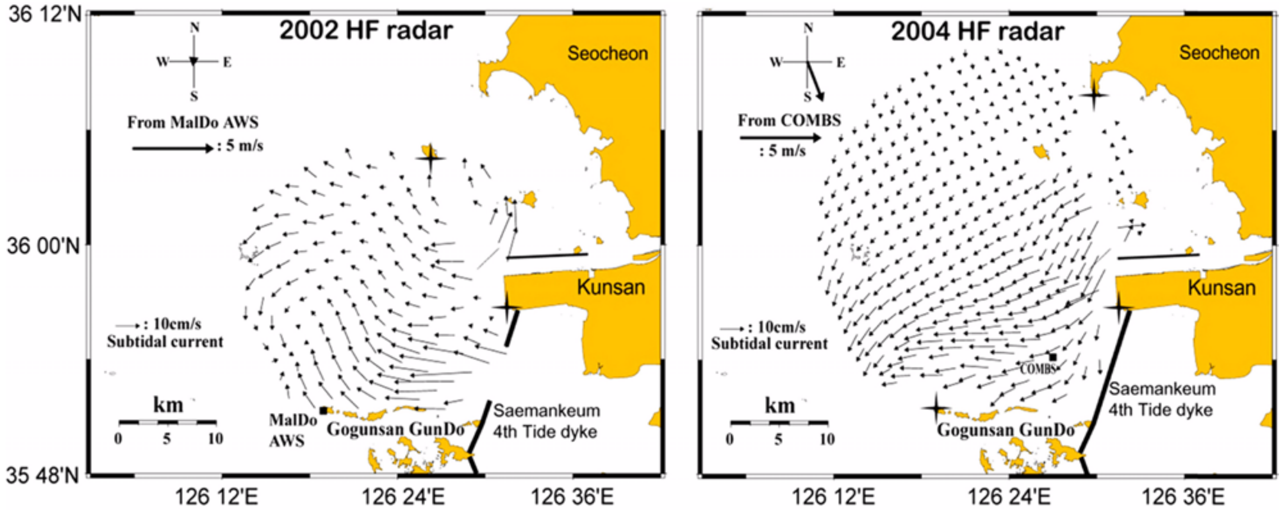

Fig. 5.3. Mean currents off the Keum River mouth in July 2002 and October 2004 (after Kim et al. 2008)

were forced primarily by the wind forcing and that the westward mean current jet from the opening in the dyke was stronger than the KRE plume current (see Figure 5.3).

After the northern dyke completion, Kim et al. (2008) showed that the prevailing northerly wind in October 2004 produced strong westward mean flows along the islands in Gogunsan-Gundo from the KRE mouth (Figure 5.3). During this period the mean deflection angle of subtidal surface currents was 71° to the right of the northerly wind, which was larger than the classical Ekman deflection. This observed angle is consistent with the deflection angle for the case of onshore wind along the straight coast as derived by Kim et al. (2009).

The SD sites also successfully captured the surface current fields off the Saemangeum southern dyke. After the dyke construction the combination of coastline configuration, wind stress and outflow jets of plume water through the gates of the two sluices modulated subtida1 surface current variability in the inner bay though variability of subtidal current in the outer bay was dominated by wind variation (Lee et al. 2013). Figure 5.4 shows that when all gates were opened in summer 2010, the easterly wind enhanced the westward expansion of subtidal surface currents. However,

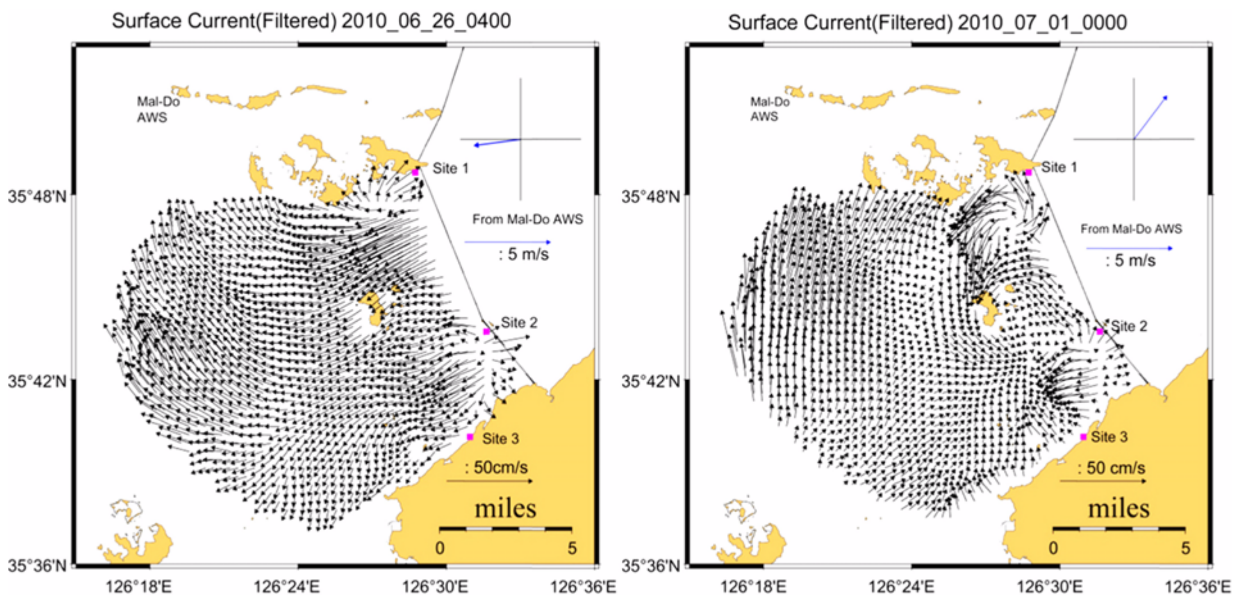

Fig. 5.4. Example of subtidal surface currents observed from three radars (CODAR, 25 MHz) in the SD sites in summer 2010 when all gates in the two sluices of the dyke were opened. The radar sites 1 and 2 are located in the jetty of the two sluices

the south-westerly wind blocked the expansion of out-flowing plume water jets, producing the counter-clockwise eddies and along-dyke flows in the inner bay.

Lee et al. (2008) examined the accuracy of radar-derived current off the KRE by comparing the facing radial vectors of two radars and with in-situ measurement currents. The root-mean-square error of the radar-derived current was smaller than 5.4 cm/s at four winter stations and 8 cm/s at two summer stations. Relevant applications of surface currents require time and space-continuous data. Hwang et al. (2011) successfully applied the objective mapping method by Kim et al. (2007) to surface currents observed by ocean radar off the KRE in order to fill in the gaps in the data.

Figure 5.5 shows typical coverage of surface current measurement, monthly mean currents and tidal current ellipses in summer by the radar observation from BNP site in Korea Strait (KHOA, 2012). The M_2 current speed increases to the Korean coast line. Mean current, indicating that TWC flows into the EJS, is stronger than the M_2 tidal current. One interesting phenomenon is a clockwise eddy in the strait when there was a low tide in Busan at 05:20, December 29, 2011. Formation mechanism and frequency of this eddy formation are under investigation.

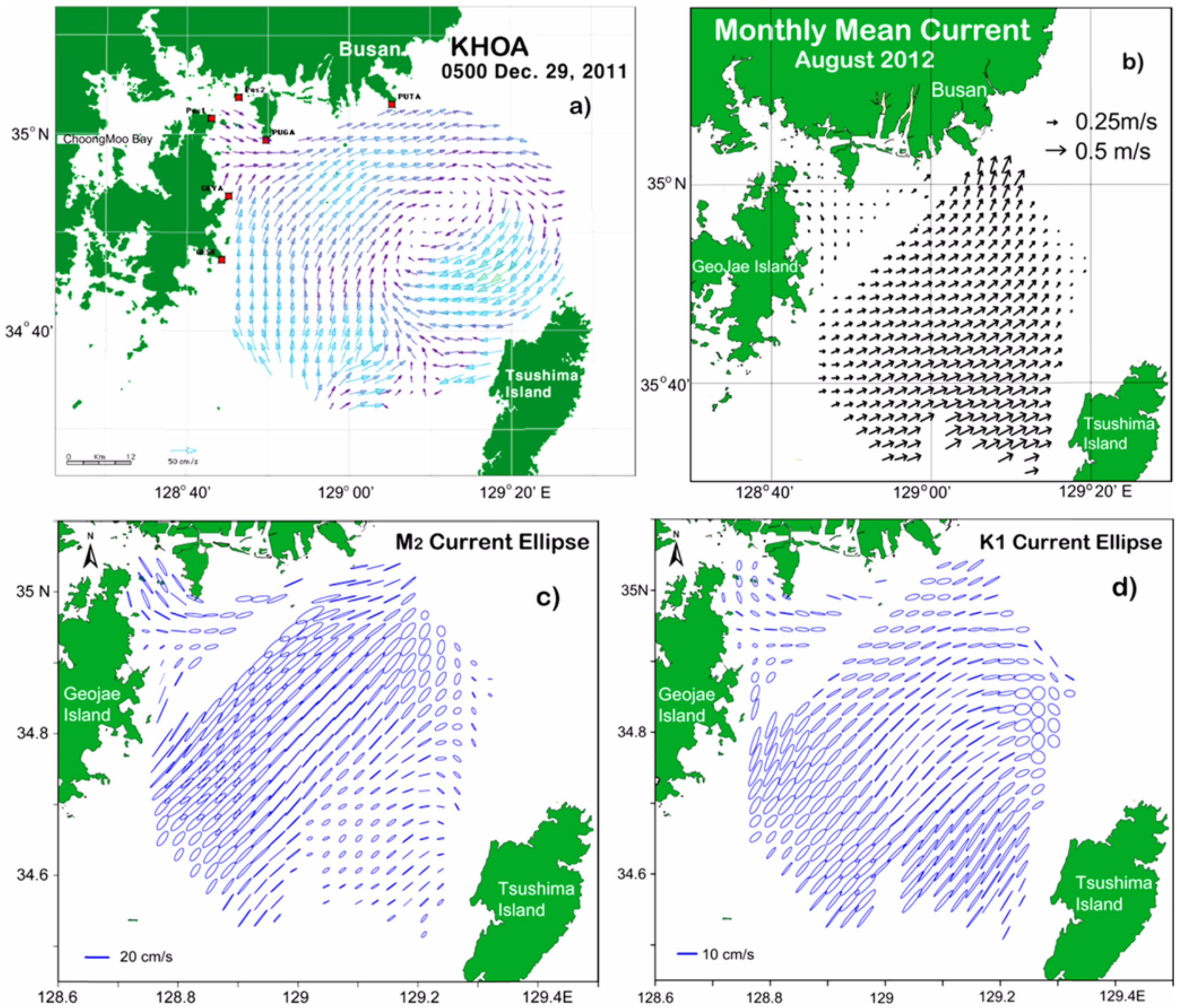

Fig. 5.5. a) Examples of surface currents in December 2011, b) monthly mean surface current, c) and d) M_2 and K_1 tidal current ellipses in August 2012 by the radar observation from BNP site in the Korea Strait

6. Ocean Radar in Taiwan

Jian-Wu Lai and Wen-Chang Yang

Introduction

Taiwan is an island and an archipelago located in the West Pacific Ocean. The strong current which is part of the North Pacific Ocean gyre called the Kuroshio flows northward past the east coast of Taiwan. It transports a variety of commercially important marine organisms in the course of completing their life histories (Mann and Lazier 2006). The Taiwan Strait is a 180 km wide strait separating the island of Taiwan from the Chinese mainland and is situated on the west side of Taiwan with the water depth less than 100 meters in most of the area. In this area, the semi-diurnal tidal current is dominant and the current direction changes rather quickly, up to four times per day. This shallow water always produces complex current velocity fields. The current field in the East China Sea north of Taiwan is influenced by the interaction of the Kuroshio and the northward current from Taiwan Strait. It is known that an important field of fishery forms under the mixing of both currents. The Luzon Strait is located south of Taiwan where a branch of the Kuroshio passes through in winter. On the whole, the ocean current velocity field around Taiwan is composed of various kinds of currents, and there are a lot of maritime activities (e.g. fishery resources and maritime transportation) in and around this area. However, due to the limitation of ocean observation technology, a long term coastal current monitoring system had not been established formerly to develop a current forecasting ability and enhance search-and-rescue performance for marine activities.

In July 2008, the Taiwan Ocean Research Institute (TORI) was established under National Applied Research Laboratories (NARL) and a 4-year ocean technology development project was launched to map surface current around Taiwan by using a network of HF ocean radars operating simultaneously. This will not only support science research because there is also the potential to provide ocean current information to assist maritime agencies and disaster mitigation responders with regard to marine salvage, oil spill response, etc. Hence, the mission to construct, operate and maintain the HF ocean radar system successfully is highly anticipated.

The establishment and maintenance of TORI HF radar system

Site scouting

In order to implement the program for setting up the CODAR SeaSonde system around Taiwan coast within four years from 2008, members of TORI CODAR team spent a lot of time on site scouting. The left side of Figure 6.1 shows the total 89 locations we have scouted. In most of these red dots, the environments have some shortcomings such as obstructions or interference of conductive materials. As a result, 11 long-range sites, marked as yellow dots in Figure 6.1, have been built. Besides, the coastline in northern and southern Taiwan is rather rugged, and the length of coastline is relatively short as well, so that the higher frequency radar is more suitable for these places to gain higher range-resolution. Consequently, 4 standard sites marked as green dots in Figure 6.1 have been constructed in these areas. Although we did some scouting in a few offshore islands, we didn’t setup any sites on them, because they are harder to approach and maintain. However, one possible consideration is for us to put additional sites on offshore islands to improve the data quality in the future since we will have more experienced operators then.

As well as a lot of red tape, those works include preliminary and detailed planning for sketching, negotiations to gain proper permission, etc. By the middle of 2012, it was very satisfying that all of the 15 HF radar sites had been successively established and were being operated with stable power supply and internet accessibility. The locations and schematic coverage of the HF ocean radar system are shown on the right side of Figure 6.1. Furthermore, a detailed field survey regarding the High Frequency RF Signal Detector must be performed before constructing a radar site. The main purposes for the detailed field survey are to verify the location for constructing the radar site to avoid as much interference from other devices as possible and provide good quality of data.

An example of administrative complexity is at the Shaioyeliou site shown on the left side of Figure 6.2, due to the ownership of the land belonging to two different government offices. After careful consideration with technicians of the manufacturer, the transmit antenna was set behind the receive antenna. This means the antennas are aligned near perpendicular to the coastline to solve the ownership problem. According to the handbook of CODAR Corporation, the antennas should be aligned parallel to the coastline. Since the energy of the signal scattered from the sea is much weaker than the transmitted one, the receive antenna was set nearer to the water than the transmit antenna. As a result, the amplitude of the backscattered signal and the signal to

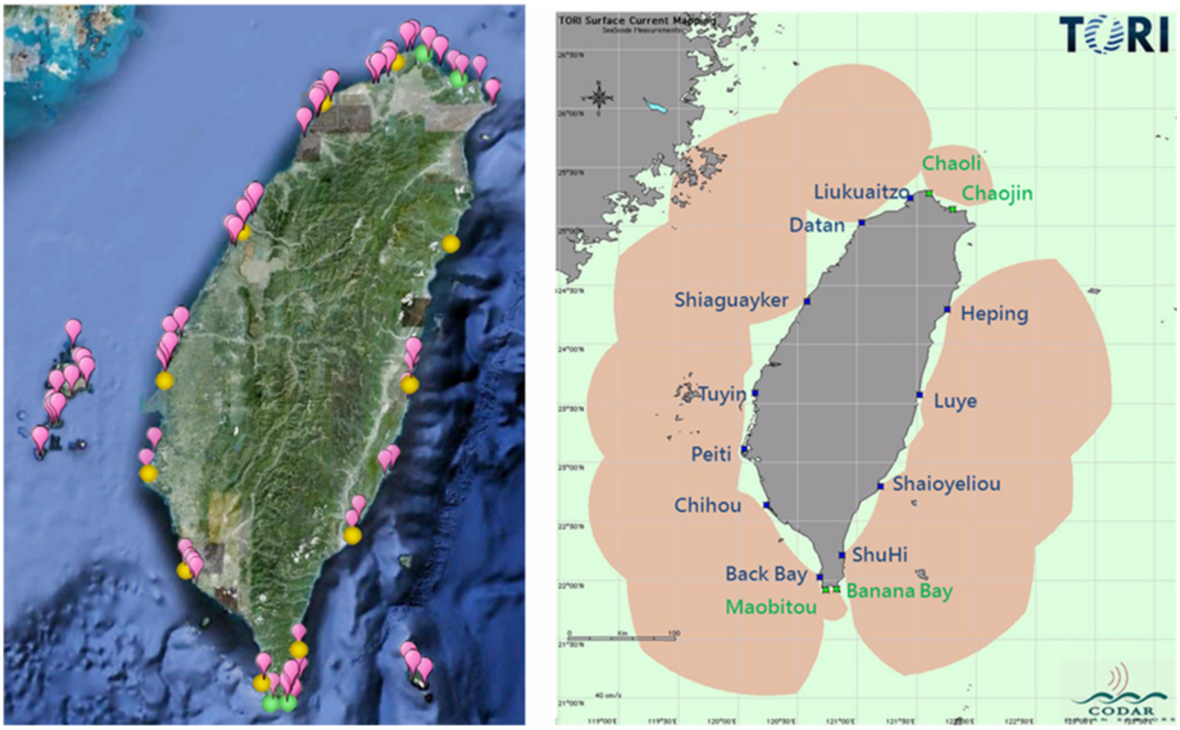

Fig. 6.1. Footprint map of site scouting and ideal coverage diagram of the TORI HF radar system

noise ratio are not obviously lower than other sites where antennas are arranged parallel to the coastline. This led to reasonable results for radial velocity measurement, as displayed on the right side of the Figure 6.2.

Internet access and site monitoring

Although most of the TORI CODAR HF radar sites are located at remote spots, fortunately, the wired internet using an Asymmetric Digital Subscriber Line (ADSL) circuit is available to access the radar sites. However, three sites are placed in remote locations that are rather hard to reach with wired internet connection. In this situation, the solution TORI adopted is a microwave Ethernet Bridge because it can transmit line-of-sight signals. Its wavelength is about one thousand times shorter than the HF radar wave so it should not interfere with the radar. According to our experience, it's rather stable and needs no maintenance. In September 2012, the last 3 sites for internet connection were setup and the HF ocean current radar network around Taiwan was completed.

In order to overcome the arduous task of taking care of a network system with fifteen sites, the real time status table for the TORI CODAR HF radar system is adopted and was modified based on the software developed by the Bodega Marine Laboratory of UC Davis. As Figure 6.3 shows, all major operation parameters of these sites are shown in one table. The site manager can see the time of the last radial file produced at each site, how many spaces are available on the root disk, how long it has been since the computer started; is the max range reduced abnormally? How hot are the electronics and what is the transmit status? Has the S/N Ratio dropped? We may know which sites need attention by the colour on the table. Take the MABT standard type site for example in Figure 6.3 where there are two red notes. The actual reason was a problem with the antenna dome, because it could not measure the radial component.

First order setting

One of the most critical features of SeaSonde analysis is the empirical determination of the frequencies that define the Bragg (first-order) region. Those factors of the first-order boundaries setting are a) threshold for noise (factor named noisefact); b) smooth the spectrum (nsm); c) find the nulls between the first- and second-order spectra (nsec, amax/fdown); d) limit the spectral range (flim); e) final frequency window (currmax) set in the 'Header' file, respectively. Factors a) b) are applied to the entire monopole self-spectrum and factors c) ~ e) are applied separately for the +ve and -ve

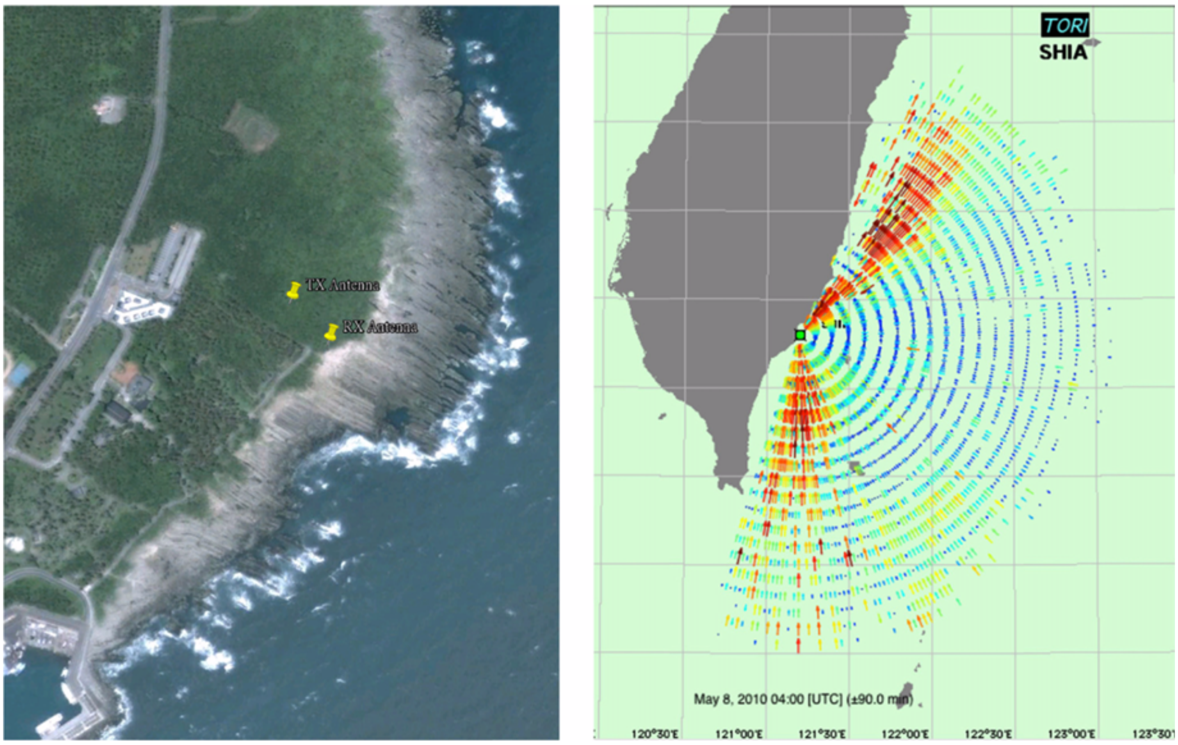

Fig. 6.2. The transmit and receive antennas was nearly perpendicular to the coastline to solve the ownership problem and the radial vector is reasonable

TORI CODAR Status Table

Updated Sun Dec 2 20:13:00 2012 UTC

Parameter	HOPE	LUYE	SHIA	SUHI	HOWN	CIHO	PETI	TWIN	TUTL	DATN	LIUK	LILY	CIAO	BABY	MABT
Last_RDLi_Short_Name	02_1800	02_1800	02_1800	02_1800	02_1800	02_1800	02_1800	02_1800	02_1800	02_1800	02_1900	02_1900	02_1900	02_1900	20_0300
Last_RDLi_Age_Hours	0	0	0	0	0	0	0	0	0	0	0	0	0	0	1768
Last_RDLm_Short_Name	02_1800	02_1800	02_1800	02_1800	02_1800	02_1800	02_1800	02_1800	02_1800	02_1800	02_1900	02_1900	02_1900	02_1900	03_0500
Last_RDLm_Age_Hours	0	0	0	0	0	0	0	0	0	0	0	0	0	0	2174
Root_Disk_Available_GB	109	160	44	33	22	151	286	63	43	81	168	29	30	278	102
Archive_Disk_Available_GB	1600	335	1361	1622	1495	1568	741	1588	838		1594	1315		1502	1979
Computer_Runtime_Hours	20	20	20	20	20	20	20	20	20	20	20	20	20	20	4
Max_Range_km	142.8	173.4	132.6	183.6	91.8	132.6	101.9	122.4	142.8	163.2	153.0	71.0	59.2	36.2	42.3
Receiver_Chassis_Temperature_DegC	25	24	29	26	28	33	31	20	29	32	28	29	26	23	28
Receiver_AWG_Temperature_DegC	36	35	38	39	42	44	43	35	40	42	40	42	40	36	41
Transmitter_Chassis_Temperature_DegC	27	25	29	25	28	35	30	19	31	34	31	29	27	22	24
Transmitter_Amplifier_Temperature_DegC	32	29	35	28	35	38	34	24	35	39	35	32	31	27	26
Transmitter_Forward_Power_W	48	58	43	46	51	48	48	53	43	53	53	43	35	52	49
Transmitter_Reverse_Power_W	3	0	0	1	2	0	3	1	3	0	0	2	4	0	0
Loop1_Phase_Deg	73.3	33.7	13.5	-140.4	-132.6	14.7	133.9	81.8	46.4	43.5	79.9	43.6	136.3	45.0	-106.7
Loop2_Phase_Deg	66.3	79.2	107.4	-118.8	-76.1	-59.3	120.1	48.1	85.2	68.9	72.8	-13.5	107.3	88.7	147.2
Monopole_SNR_dB	-44.	-40.	-30.	-42.	-34.	-35.	-39.	-36.	-42.	-34.	-31.	-32.	-32.	-36.	-46.
Sentinel_Log_Failures	1	1	1	64	1	8	17	3	3	1	3	12	37	63	17

Fig. 6.3. Real-time Status Table for TORI HF radar network which was modified based on the software developed by Bodega Marine Laboratory of UC Davis

Doppler halves of the monopole self-spectrum (CODAR Ocean Sensors, 2009). A frequency window is applied to the Doppler spectrum, so the derived current speed will not exceed the value 'currmax', which is the maximum current

Table 6.1. Summary of currmax setting for 15 CODAR SeaSonde sites

Area	South	North	East	West
Station	BABY, MABT	CIAO, LILY	SUHI, SHIA, LUYE, HOPE	HOWN, CIHO, PETI, TWIN, LIUK, DATN, TUTL
Freq. (MHz)	24.3	13.425	4.58	4.58
BW (kHz)	-99.259	-99.259	-40.439	-40.439
Currmax (m/s)	1.8 2.0	1.8	2.6	1.5 1.5 1.5 1.8 1.5 1.5 1.5

estimated for the geographical location of the radar.

As we mentioned in the introduction, the ocean currents that surround Taiwan Island have different characteristics with regard to the east coast and the west coast, i.e., the east coast is mainly dominate by the Kuroshio current but in the west coast (Taiwan strait) the currents are complex and protean due to the mixed tide and monsoon. These lead to fluctuations which are in the order of the average current velocities. At present, we may only estimate the maximum current in the radar monitoring area based on the velocity field of the historical data obtained by Sb-ADCP moorings and released by Ocean Data Bank, National Science Council, Taiwan, and based on summarizing the data from the questionnaire survey of oceanographic experts. Therefore, the TORI CODAR team setup the 'currmax' values (1.5~ 2.6 m/sec) for 15 radial sites in different areas (as list in Table 6.1). Another challenge to the data quality comes from the ionospheric interference that may affect the noise floor and signal to noise ratio daily. As the Figure 6.4 shows, the noise floor varies from -65 dBm to -75 dBm between 0800h to 2300h. Furthermore, a long-term statistical analysis of maximum Doppler shift and threshold of noise interference within the monopole self-spectrum for each site is being undertaken to robustly establish the first-order boundaries setting.

The data archive

There are many advantages of the HF radar detecting method over other measurement methods, such as large spatial coverage, near real-time, high spatial resolution, low-cost, and the capability of working at all-times and under all-weather conditions (Barrick et al. 1977). It is pleasing and encouraging for TORI's CODAR team that the establishment of all the 15 radar sites has been completed within the past four years as scheduled. Upon cautious implementation and operation of HF radar sites, TORI has come to appreciate, understand, confront, and solve several issues that have risen. For the TORI HF ocean radar network, radial data are transferred from 15 stations to a control center in TORI headquarters through the internet and combined to get the surface current vectors on a 10-km square grid according to the least square fit. The surface current map around Taiwan is archived hourly. Up to the present, the surface current

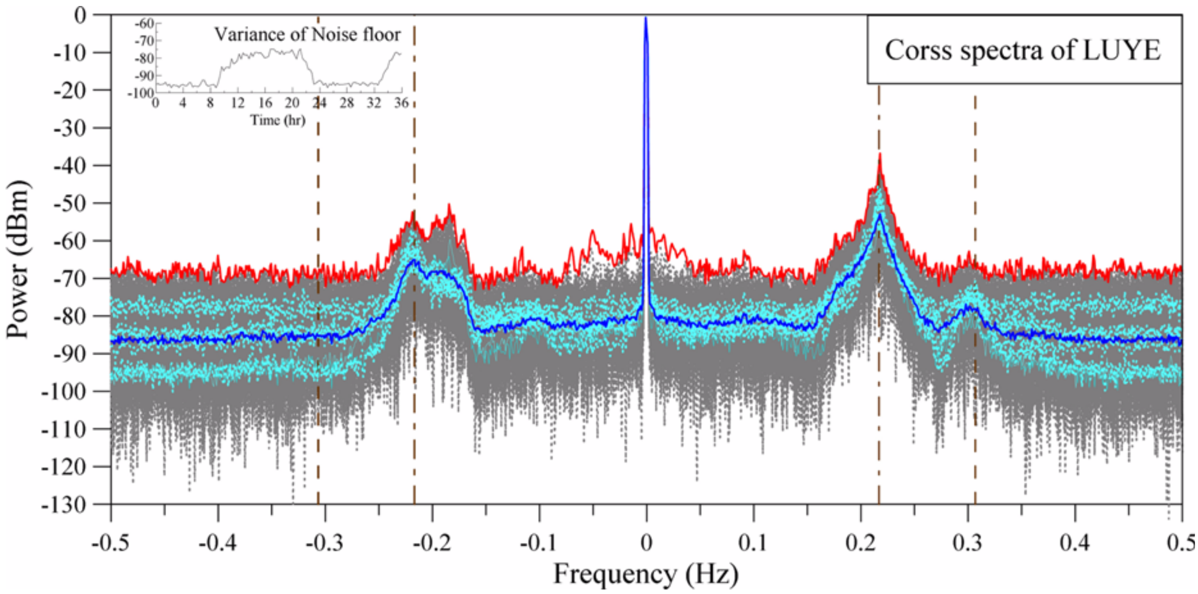

Fig. 6.4. Characteristics of variation and statistic of CSQ spectra at LUYE station in 36 hours

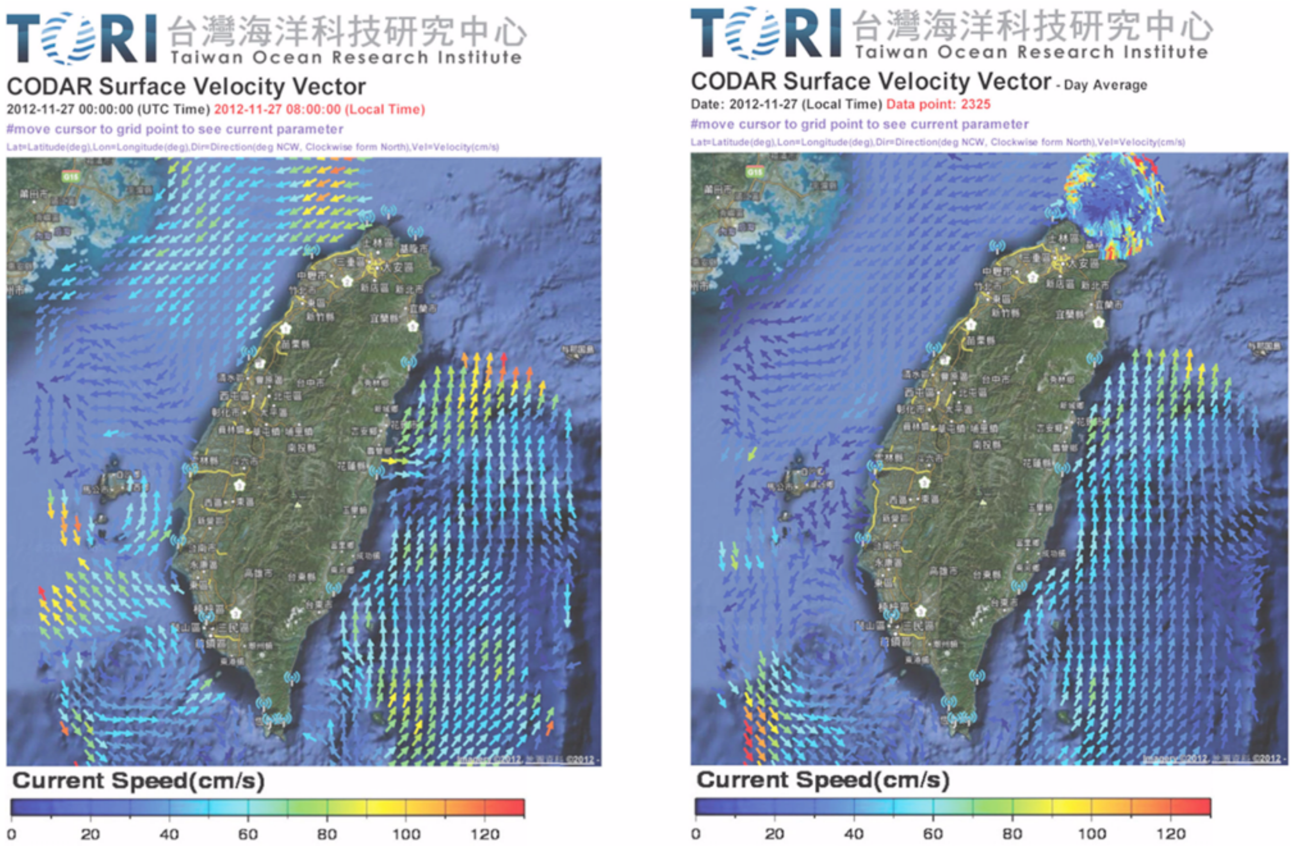

Fig. 6.5. An example of hourly and daily average current map of TORI HF ocean radar network

map data released by the TORI CODAR team are processed using factory software and no additional quality control has been carried out on these data.

As Figure 6.5 demonstrates, the near real-time hourly and daily average current maps can be viewed on the Marine Environmental Databank (MED) found at http://med.tori.org.tw/CODAR/.

7. Summary

Kuh Kim and Sang-Ho Lee

This overview paper, composed of sections for five regions in Asia and Oceania, introduces the diverse history and focus of their oceanographic radar network developments, mainly depending on the characteristics of coastal regions in individual countries. Australia and Taiwan, surrounded by open seas, have developed mostly long range radar networks along their relatively simple coast lines to monitor major ocean currents, interactions between physical parameters and ecology, and to provide information for disaster mitigation. On the other hand, Japan and Korea have many bays, inland seas and straits, so that standard range radar networks are common to support marine safety and management of coastal seas as well as to study ocean current dynamics. It is noted that China and Japan made big efforts to develop their own radar systems. Though the radar networks of Vietnam, Thailand and Indonesia have not been introduced in this paper, their radar networks have been known to mainly detect the typhoon and tsunami attacks.

Australia and Taiwan have their own nation-wide systems of managing, integrating and archiving data from the radars; ACORN and TORI. Korea has fostered the radar community by forming the Korea Ocean Radar Forum; Japan has held an annual workshop to address all issues raised by operators and end-users; and the first regional Ocean Radar Conference for Asia (ORCA), which inspired this Special Issue, was held in Korea in 2012.

Highlights of research and application using oceanographic radars depend on the goals and operational experiences of the radar network in each country. Australia has shown its capability with regard to the phased-array system, with its good temporal and spatial resolution, to track individual water parcels including pollutants when the coal carrier ran aground on Douglas Shoal in the southern Great Barrier Reef in 2010. China has demonstrated the applicability of their own radars to trace typhoon centers and has introduced experiments to measure the water depths in shallow water by figuring out the Bragg wave's phase velocity biases from its deep water value. Japan first demonstrated the tsunami detection ability of oceanographic radars at a distance of 12 km from the shore in Kii Channel at a range of about 1000 km from the epicenter of the Tohoku earthquake on March 11, 2011. Korea showed that the radar successfully monitors changes in coastal circulation caused by the large coastal development of the Saemangeum project in the macro tidal environment of the western Yellow Sea. Despite the young age of the radar network, Taiwan is the first country in Asia that has completed a nation-wide radar network by covering all coastal seas around the country from 2008 to 2012.

China, Japan, Korea and Taiwan operated 81% of oceanographic radars in Asia and Oceania. As these countries share the Pacific marginal seas and narrow straits between them, this overview paper may contribute as the first step to promote regional collaborations in radar observations, data usages and applications in order to efficiently monitor the coastal and marginal sea waters along the western Pacific Ocean periphery, study ocean current dynamics and ecology, and support marine safety and tsunami detection.

Acknowledgements

The Australian work forms part of the Integrated Marine Observing System (IMOS) within the National Collaborative Research Infrastructure Strategy (NCRIS) in Australia and all radar data are from the IMOS archive. The Australian Institute of Marine Science supports this work. The Korean authors were supported by the Korea Meteorological Administration Research and Development Program under Grant CATER 2012-2080. The work in Taiwan forms part of the Ocean Technology Development Project within the Taiwan Ocean Technology Institute (TORI), National Applied Research Laboratories (NARL) and is funded by National Science Council, Republic of China. Administrative support was provided by Coast Guard Administration (ROC), Navy (ROC), Kenting National Park Administration, East Coast National Scenic Area Administration, Hoping Industrial Harbor Administration, and Taiwan Power Company.

References

Barrick DE, Evans MW, Weber BL (1977) Ocean surface current mapped by radar. Science **198**:138-144

Barrick DE (1977) Extraction of wave parameters from measured HF radar sea-echo Doppler spectra. Radio Sci **12**:415-424

Barrick DE, Lilleboe PM, Teague CC (2001) Multi-station HF FMCW radar frequency sharing with GPS time modulation multiplexing. U.S. Patent 6 856 276

Choi BH (1980) A tidal model of the Yellow Sea and the Eastern China Sea. KORDI Report 80-02, 72 p

Choi SB, Kim HS, Moon JY, Lee KH, Ogasawara I, Kniehoff M (2012) Test results of array type HF radar in the eastern coast of Korea. In: Proceeding of the 1st Ocean Radar Conference for Asia (ORCA), **SP-2**, pp 96-99. http://korf.kunsan.ac.kr/Doc_Forms/P_A_3.pdf

CODAR Ocean Sensors (2002) Defining first-order region boundaries. Mountain View, California, 9 p

Crombie DD (1955) Doppler Spectrum of Sea Echo at 13.56 Mc/s. Nature **175**:681-682

Ebuchi N, Fukamachi Y, Oshima K, Shirasawa K, Ishikawa M, Takatsuka T, Daibo T, Wakatsuchi M (2006) Observation of the Soya warm current using HF ocean radar. J Oceanogr **62**(1):47-61

Fujii S, Sato K, Matsuoka T, Kojima S (2003) The HF ocean radar for current observation at the southern part of East China Sea. In: The 12th PAMS/JECSS workshop, Hangzhou China, No.12-1

Fujii S, Tokuda M (1996) Tsunami and ocean monitoring and forecasting system. Japanese Patent 2721486 (In Japanese)

Hashimoto N, Wyatt L, Kojima S (2003) Verification of a Bayesian method for estimating directional spectra from HF radar surface backscatter. Coast Eng J **45**(2):255-274

Hasselmann K (1971) Determination of ocean wave spectra from Doppler radio return from the sea surface. Nat Phys Sci **229**:16-17

Heron ML (1985) Line broadening of HF ocean surface radar backscatter spectra. J Oceanic Eng **10**:397-401

Heron ML, Dexter PE, McGann BT (1985) Parameters of the air-sea interface by HF ground-wave Doppler radar. Aust J Freshw Mar Res **36**:655-670

Heron ML, Mantovanelli A, Steinberg C, King B (2010) What can HF radar contribute to the salvage of a grounded ship? In: IEEE/MTS OCEANS 2010, Seattle, IEEE Xplore

Heron ML, Wyatt LR, Atwater DP, Prytz A (2012) The Australian Coastal Ocean Radar Network: Lessons learned in the establishment phase. In: IEEE/MTS OCEANS 2012 Yeosu, Korea, IEEE Xplore

Hinata H, Fujii S, Furukawa K, Kataoka T, Miyata M, Kobayashi T, Mizutani M, Kokai T, Kanatsu N (2011) Propagating tsunami wave and subsequent resonant response signals detected by HF radar in the Kii Channel, Japan. Estuar Coast Shelf Sci **95**:268-273

Hinata H, Yanagi T, Takao T, Kawamura H (2005) Wind-induced Kuroshio warm water intrusion into Sagami Bay. J Geophys Res **110**:C03023. doi:10.1029/2004JC002300

Hisaki Y (1996) Nonlinear inversion of the integral equation to estimate ocean wave spectra from HF radar. Radio Sci **31**(1): 25-39

Hou J-C, Wu S-C, Yang Z-J, Qiu C-R, Wen B-Y Shi Z-H, Wu Q-L, Guan R-S, Wang S-R (1997) Remote sensing of ocean surface currents by HF radar. Chinese J Geophys **40**(1):18-26

Hwang J-A, Lee S-H, Choi B-J, Kim C-S (2010) Application of objective mapping to surface currents observed by HF radar off the KR estuary. J Korean Soc Oceanogr (The Sea) **15**(1):42-55

Ichikawa K, Tokeshi R, Kashima M, Sato K, Matsuoka T, Kojima S, Fujii S (2008) Kuroshio variations in the upstream region as seen by HF radars and satellite altimetry data. Int J Remote Sens **29**(21):6417-6426

IOOS, NOAA (2009) A plan to meet the nation's needs for surface current mapping. 33 p

ITU (2012) Final acts of the World Radiocommunication Conference (WRC-12). Geneva, pp 490

KHOA (2012) Monthly report of Korea oceanographic observation network. 11-1611234-000209-06, pp 168

Kim CS, Lee SH, Son YT, Kwon HK, Lee KH, Kim YB, Jeong OJ (2006) Changes of surface M_2 currents as observed by HF radar before and after Saemangeum forth tidal dyke closing. J Korean Soc Oceanogr (The Sea) **11**:37-48

Kim CS, Lee SH, Son YT, Kwon HK, Lee KW, Choi BJ (2008) Variations in subtidal surface currents observed with HF radar in the coastal waters off the Saemangeum area. J Korean Soc Oceanogr **13**(1):56-66 (In Korean)

Kim DH, Hong HB, Lee YS, Hong SD (2012) On the accuracy of HF radar surface current measurements in the south sea of Korea. In: Proceeding of the 1st Ocean Radar Conference for Asia (ORCA), **S2-4**, pp 49

Kim K, Kim K-R, Min D-H, Volkov Y, Yoon J-H, Takematsu M (2001) Warming and structural changes in the East (Japan) Sea: A clue to future changes in global oceans? Geophys Res Lett **28**:3293-3296

Kim SY, Terrill EJ, Cornuelle BD (2007) Objectively mapping HF radar-derived surface current data using measured and idealized data covariance matrices. J Geophys Res **112**:C06021. doi: 10.1029/2006JC003756

Kim SY, Cornuelle BD, Terrill EJ (2009) Anisotropic response of surface currents to the wind in a coastal region. J Phys Oceanogr **39**:1512-1533. doi:10.1175/2009JPO4013.1

Lee JH, Kim JH, Chong (2012) Frequency allocation for oceanographic radars and review of their usage in the radio interference aspects. In: Proceeding of the 1st Ocean Radar Conference for Asia (ORCA), **SP-4**, pp 101-104

Lee S-H, Choi HY, Son YT, Kwon HK, Kim YK, Yang JS (2003) Low-salinity water and circulation in summer around the Saemangeum area in the west coast of Korea. J Korean Soc Oceanogr (The Sea) **8**(2):138-150

Lee S-H, Moon HB, Baek HY, Kim CS, Son YT, Kwon HK, Choi BJ (2008) On the accuracy of current measurement by HF radar in the coastal sea off the Keum River estuary. J Korean Soc Oceanogr (The Sea) **13**(1):42-55

Lee S-H, Kang CY, Choi BJ, Kim CS (2013) Surface Subtidal Current Response to Wind and Plumes during summer 2010 in a Bay-shape Estuary of the eastern Yellow Sea: Ocean Radar Observation. Ocean Sci J **48**(1):117-139

Lipa BJ, Nyden B, Ullman DS, Terrill E (2006) SeaSonde radial velocities: Derivation and internal consistency. IEEE J Oceanic Eng **31**(4):850-861

Morimoto A, Kojima S, Jan S, Takahashi D (2009) Movement of the Kuroshio axis to the northeast shelf of Taiwan during typhoon events. Estuar Coast Shelf Sci **82**:547-552

Nadai A, Kuroiwa H, Mizutori M, Sakai S (1999) Measurement of ocean surface currents by the CRL HF ocean radar of FMCW type, Part 2 current vector. J Oceanogr **55**(1):13-30

Ohno Y (1991) HF ocean radar observations of ocean currents. J Commun Res Lab **38**(3):377-385

Ramp S, Barrick D, Ito T, Cook M (2008) Variability of Kuroshio current south of Sagami bay as observed using long-range coastal HF radar. J Geophys Res **113**:C06024. doi:10.1029/2007JC004132

Sakai S, Tsubono T, Matsuyama M, Muzunuma M (2003) Coastal current observation in the area of abrupt topographic change with DBF radar. In: IEEE IGARSS, Toulouse, France, pp 1852-1855

Son YT, Lee SH, Kim CS, Lee JC, Lee GH (2007) Surface current variability in the KR Estuary (South Korea) during summer 2002 as observed by high-frequency radar and coastal monitoring buoy. Cont Shelf Res **27**:43-63

Son YT, Kim K, Chang KI (2012) Operation of HF radar on the east coast of Korea. In: Proceeding of the 1st Ocean Radar Conference for Asia (ORCA), SP-1, pp 92-95

Song KM, Cho CH, Jung KT, Park JS, Lie HJ (2012) Application of HF radar to observation of surface current fields in the Cheju Strait, Korea. In: Proceeding of the 1st Ocean Radar Conference for Asia (ORCA), SP-3, pp 100

Takahashi D, Guo X, Morimoto A, Kojima S (2009) Biweekly periodic variation of the Kuroshio axis northeast of Taiwan as revealed by ocean high-frequency radar. Cont Shelf Res **29**: 1896-1907

Takeoka H, Tanaka Y, Ohno Y, Hisaki Y, Nadai A, Kuroiwa H (1995) Observation of the Kyucho in the Bungo channel by HF radar. J Oceanogr **51**(6):699-711

Yoshikawa Y, Masuda A, Marubayashi K, Ishibashi M (2010) Seasonal variations of the surface currents in the Tsushima strait. J Oceanogr **66**(2):223-232

Yoshikawa Y, Masuda A, Marubayashi K, Ishibashi M, Okuno A (2006) On the accuracy of HF radar measurement in the Tsushima Strait. J Geophys Res **111**:C04009. doi: 10.1029/2005JC003232

You HY, Huh Y, Lee SL, Han KN (2012) Management and future plans for Korea HF radar network. In: Proceeding of the 1st Ocean Radar Conference for Asia (ORCA), S1-7, pp 33-35

Wu X, Li Y (2012) Estimates of drag coefficient over the Taiwan Bank using HF-Radar system. In: Proceeding of the 1st Ocean Radar Conference for Asia (ORCA), Seoul, Korea

Wu X, Yang S, Cheng F, Wu S, Yang JI, Wen B, Shi Z, Tian J, Hou J, Ke H, Gao H (2003) Ocean surface currents detection at the Eastern China Sea by HF surface wave radar. Chinese J Geophys **46**(3):340-346

Wu X-B, Li L, Li Y, Long C, Shen Z-B, Yang Z-J (2012) Experimental research on significant wave height detection with HFSWR OSMAR071. Oceanol Et Limnol Sin **43**(2):210-216

Wyatt LR, Green JJ, Middleditch A (2011) HF radar data quality requirements for wave measurement. Coast Eng **58**:327-336

Wyatt LR (2012) Shortwave direction and spreading measured with HF radar. J Atmos Ocean Tech **29**:286-299

Zhang Z (2009) Studies on Computation of the Three-Dimensional Hydrodynamic Parallel Model. Ph.D. Thesis, Xiamen University, p 157

Zhu D, Shao H, Li Y, Li L (2007) Quality analyses of radial currents measured by a demonstration system of OSMAR HF radar in Fujian Province. J Oceanogr Taiwan Strait **26**(1):7-16

Zhu DY, Li L, Li Y, Guo XG (2008) The Taiwan Strait South-west of the seasonal variation of surface currents by HF ground wave radar observation. Chinese Sci Bull **53**(11):1339-1344